

Sustainable Synthesis of Schiff Base Derivatives via Ionic Liquid and Microwave-Assisted Approach: Structural, Biological, and Computational Evaluation

Nilesh Bhusari[#], Abhay Bagul^{b#}, Vipin Kumar Mishra^c, Aisha Tufail^d, Digambar Gaikwad^{b*} and Amit Dubey^{e*}

^a Department of Chemistry, Maulana Azad College of Arts, Science and Commerce, Chhatrapati Sambhajinagar 431004, Maharashtra, India

^b Department of Forensic Chemistry, Government Institute of Forensic Sciences, Chhatrapati Sambhajinagar 431004, Maharashtra, India

^c Chemistry Division, School of Advanced Sciences and Languages, VIT Bhopal University, Bhopal, India

^d Computational Chemistry and Drug Discovery Division, Quanta Calculus, Greater Noida-201310, Uttar Pradesh, India

^e Center for Global Health Research, Saveetha Medical College and Hospital, Saveetha Institute of Medical and Technical Sciences, Chennai-600077, Tamil Nadu, India

***Corresponding Authors:**

Digambar Gaikwad, Department of Forensic Chemistry, Government Institute of Forensic Sciences, Chhatrapati Sambhajinagar 431004, Maharashtra, India

Email Address: gaikwad.dd.dg@gmail.com

Amit Dubey, Center for Global Health Research, Saveetha Medical College and Hospital, Saveetha Institute of Medical and Technical Sciences, Chennai-600077, Tamil Nadu, India

Email address: ameetbioinfo@gmail.com, amitdubey@saveetha.com

#_Equal Contribution

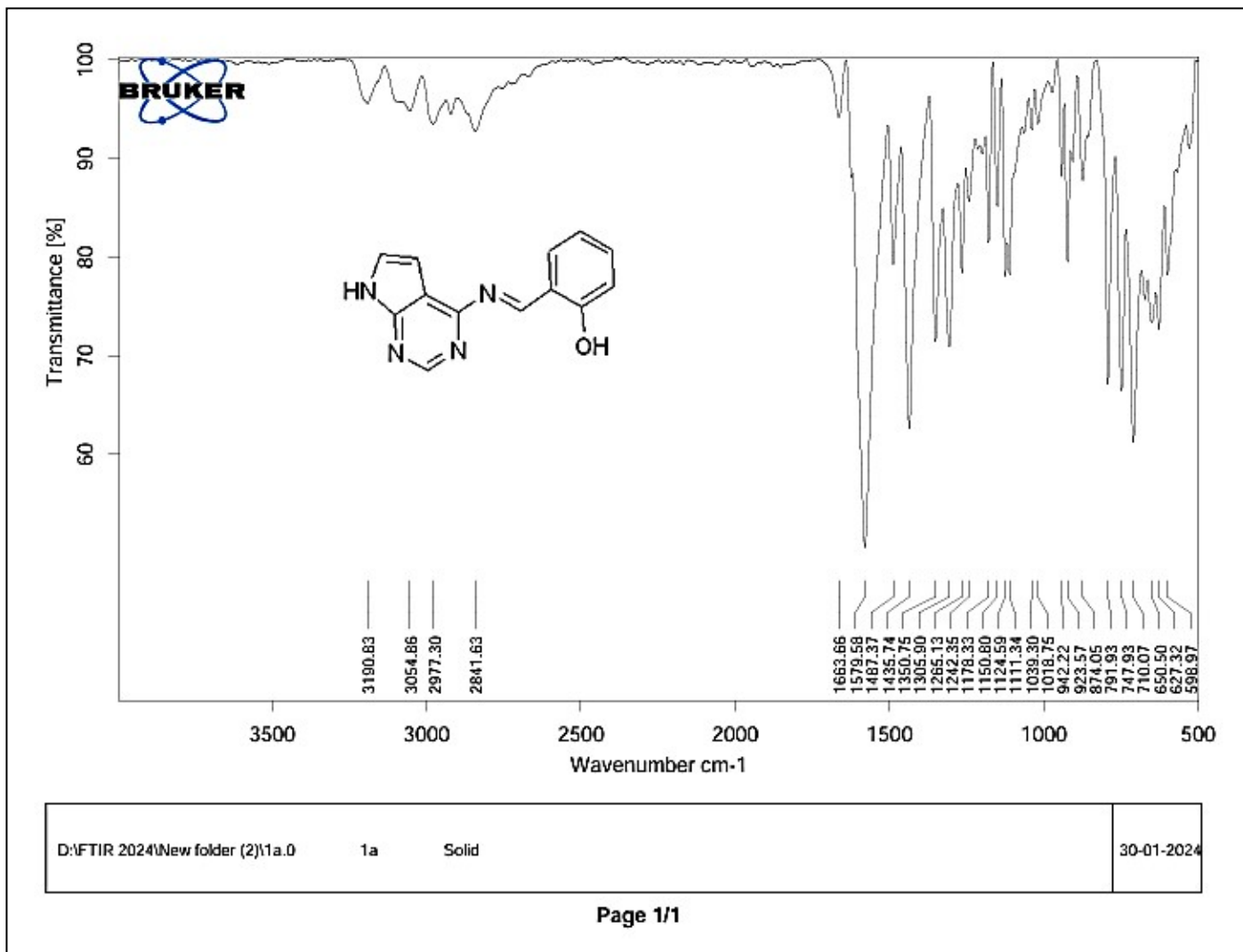


Figure. S1 IR spectrum of APR1a

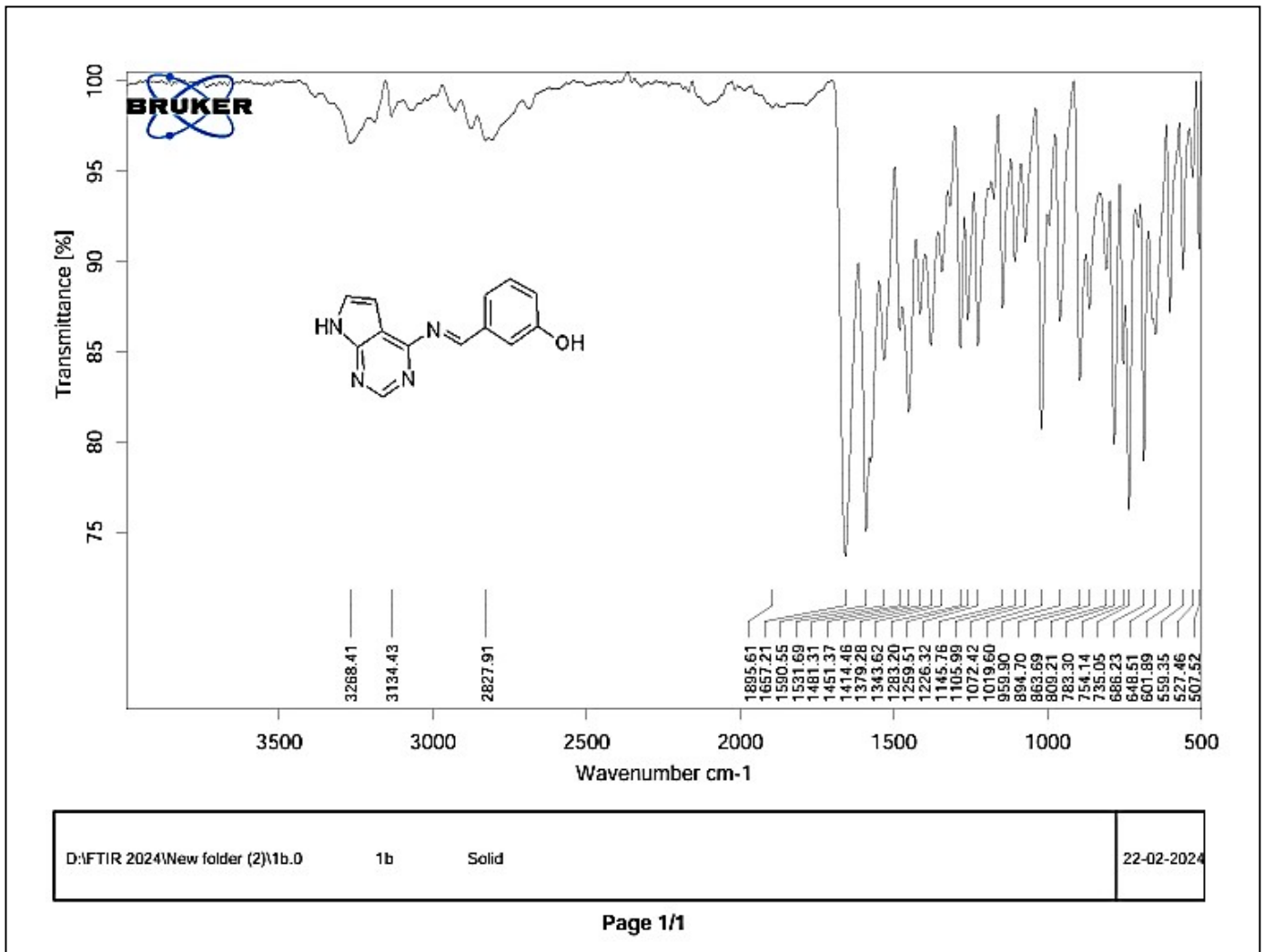


Figure. S2 IR spectrum of APR1b

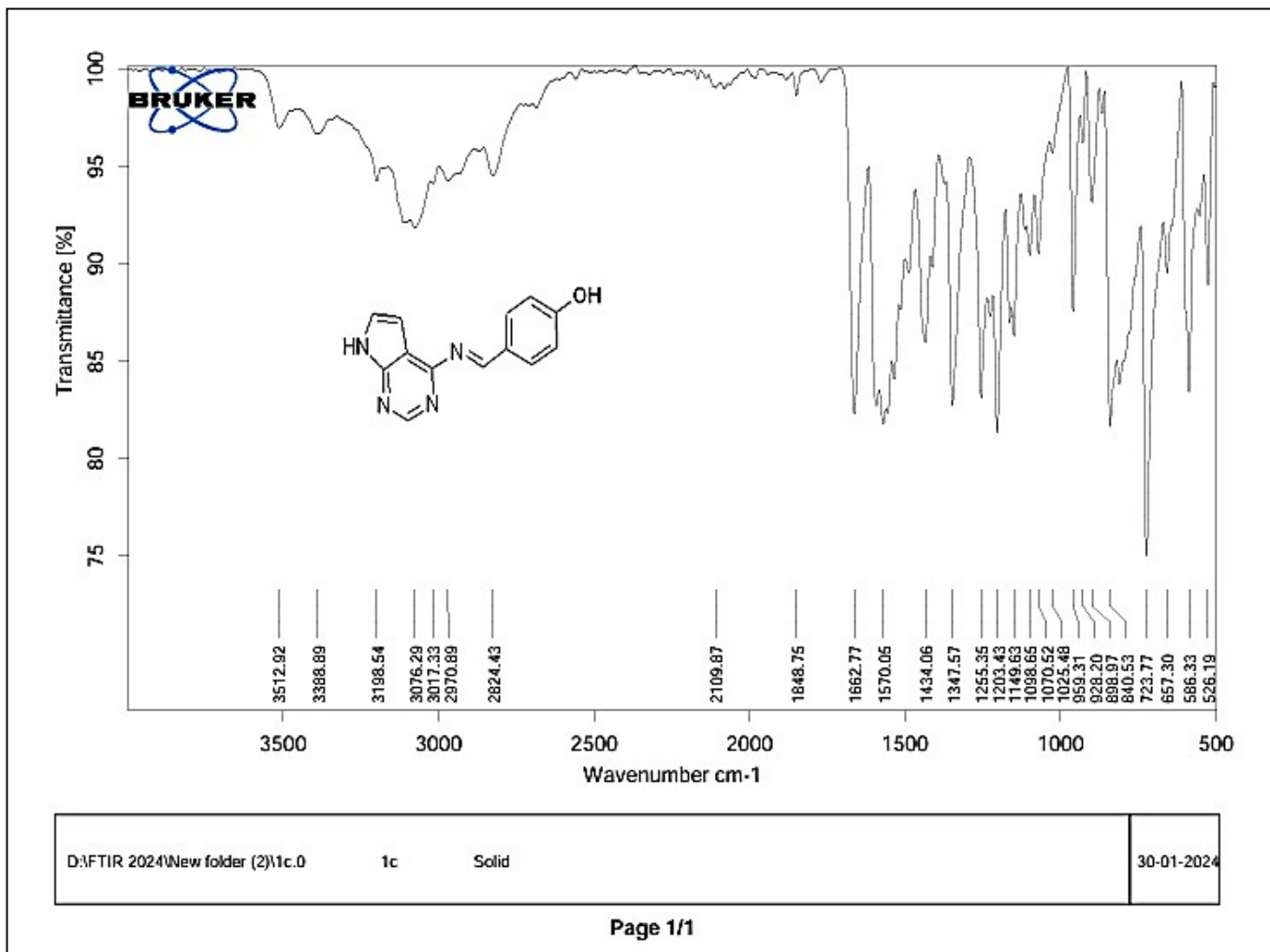


Figure. S3 IR spectrum of APR1c

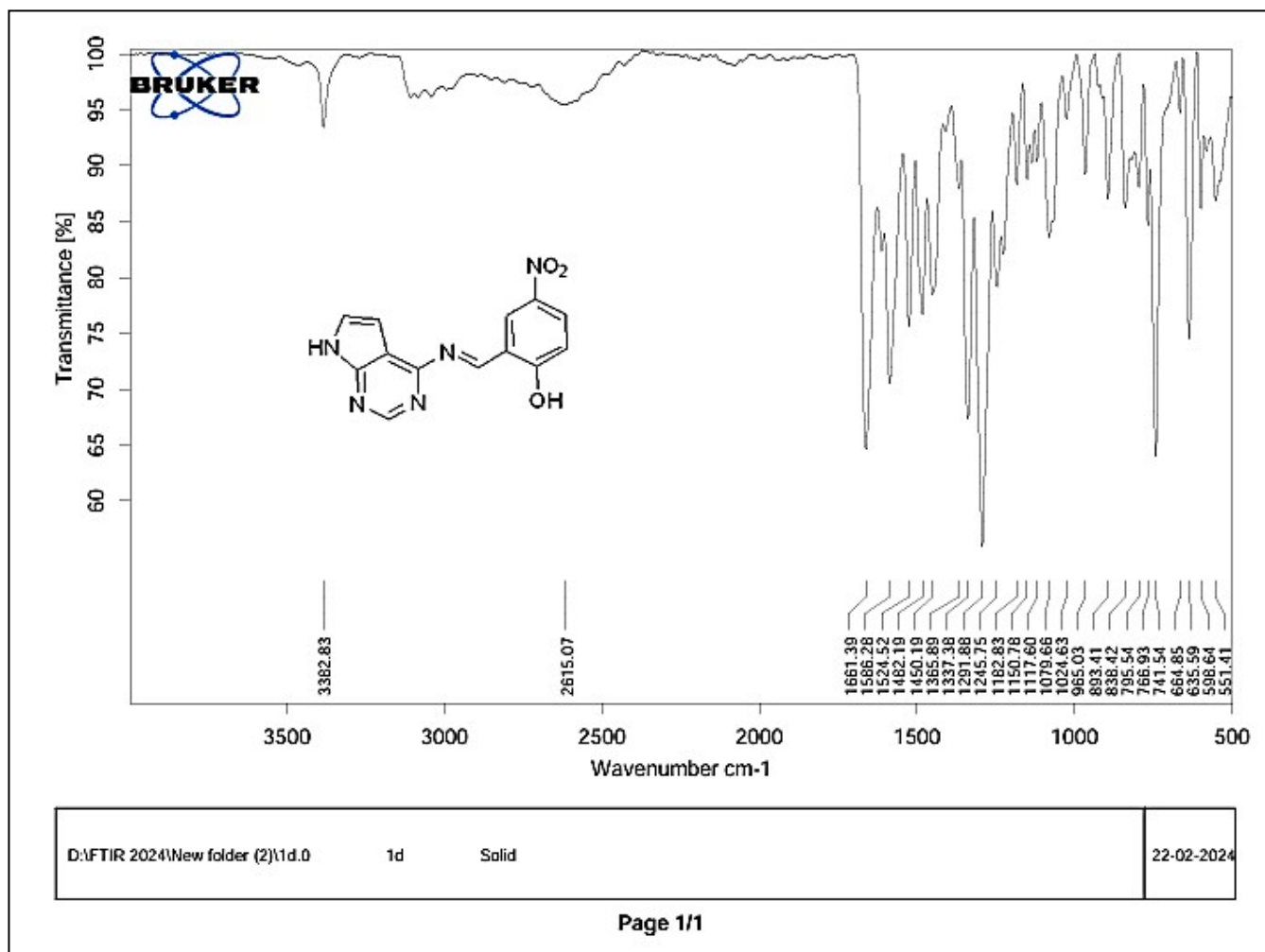


Figure. S4 IR spectrum of APR1d

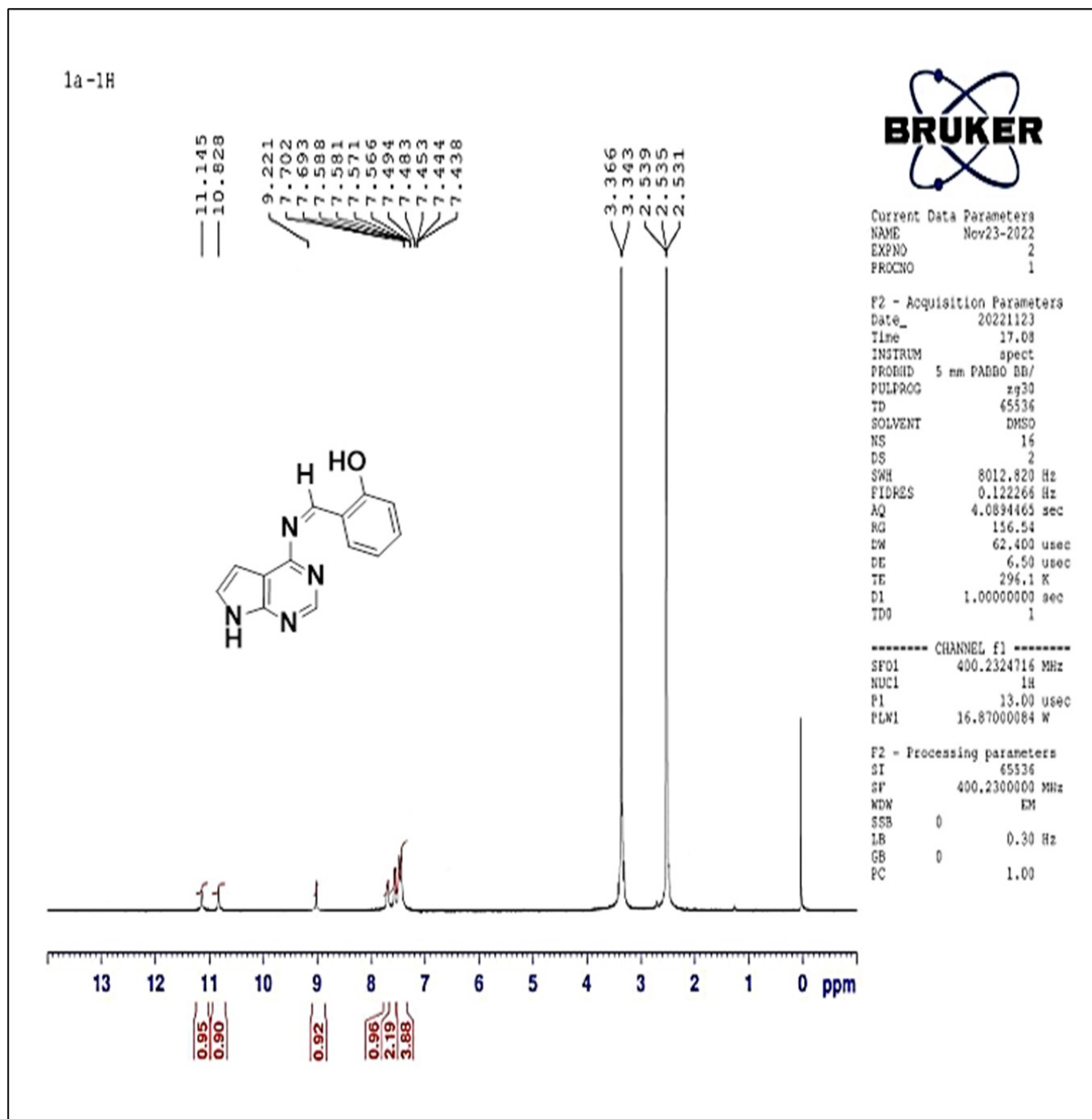


Figure. S5 ^1H NMR (400 MHz in DMSO-d_6) of the Compound APR1a : δ 11.145 (Ar-NH), δ 10.828 (Ar-OH), δ 9.221 (Ar-CH=NH), δ 7.438-7.702 (Ar-CH) ppm.

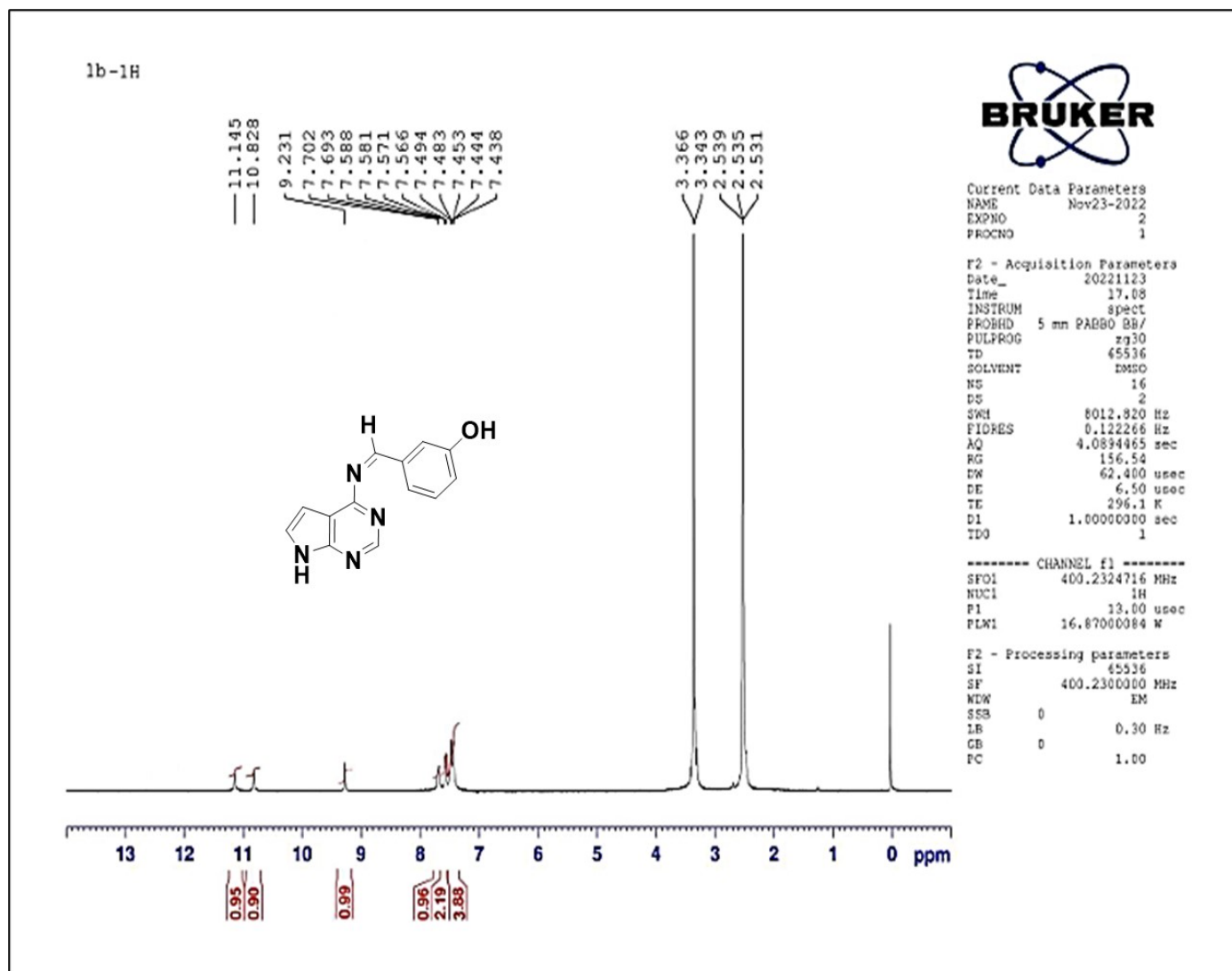


Figure. S6 ^1H NMR (400 MHz in DMSO-d_6) of the Compound APR1b: δ 11.145 (Ar-NH), δ 10.828 (Ar-OH), δ 9.231 (Ar-CH=NH), δ 7.438-7.702 (Ar-CH)

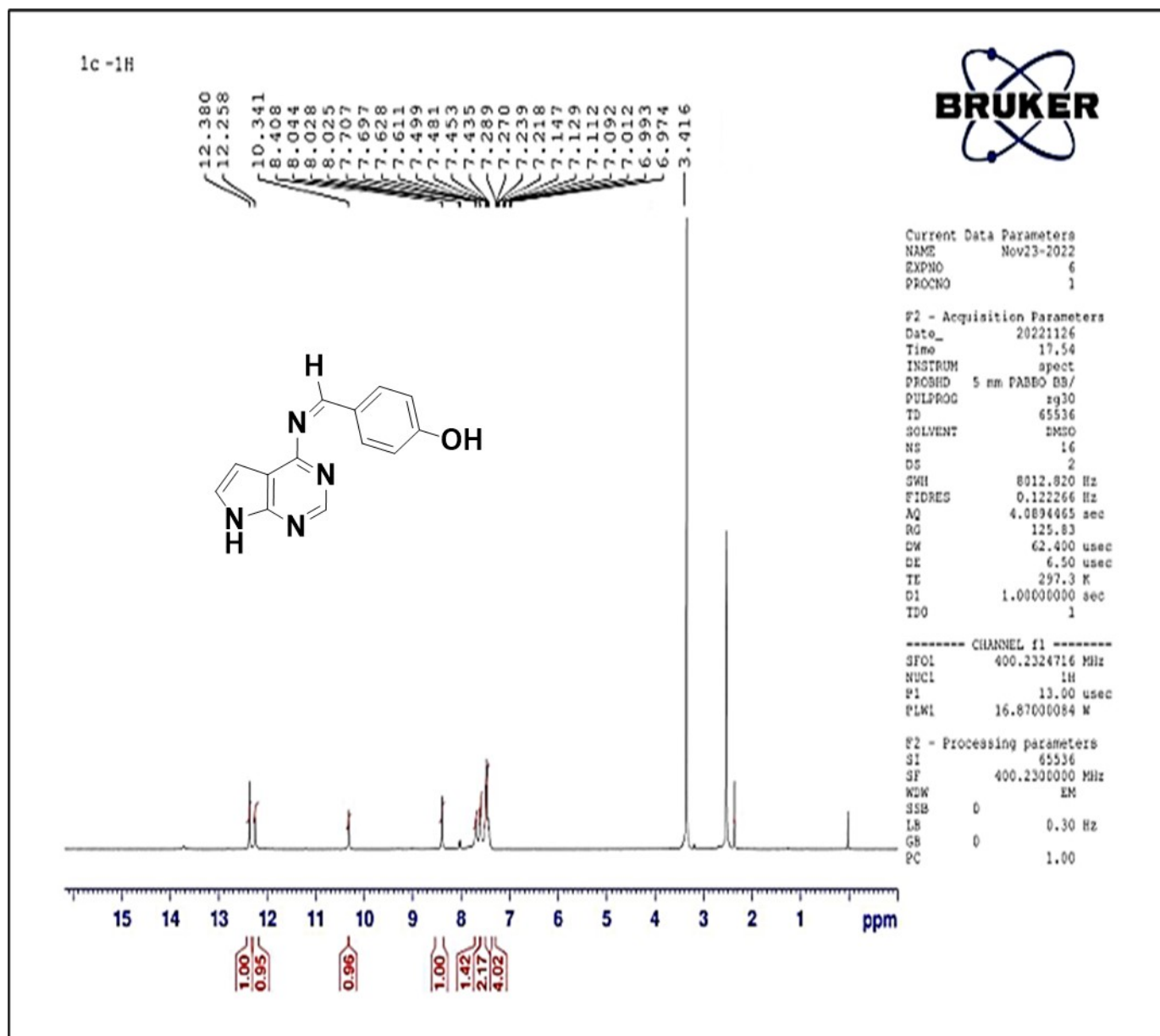


Figure. S7 ^1H NMR (400 MHz in DMSO-d_6) of the Compound APR1c: δ 12.38 (Ar-NH), δ 12.258 (Ar-OH), δ 10.341 (Ar-CH=NH), δ 6.974-8.408 (Ar-CH)

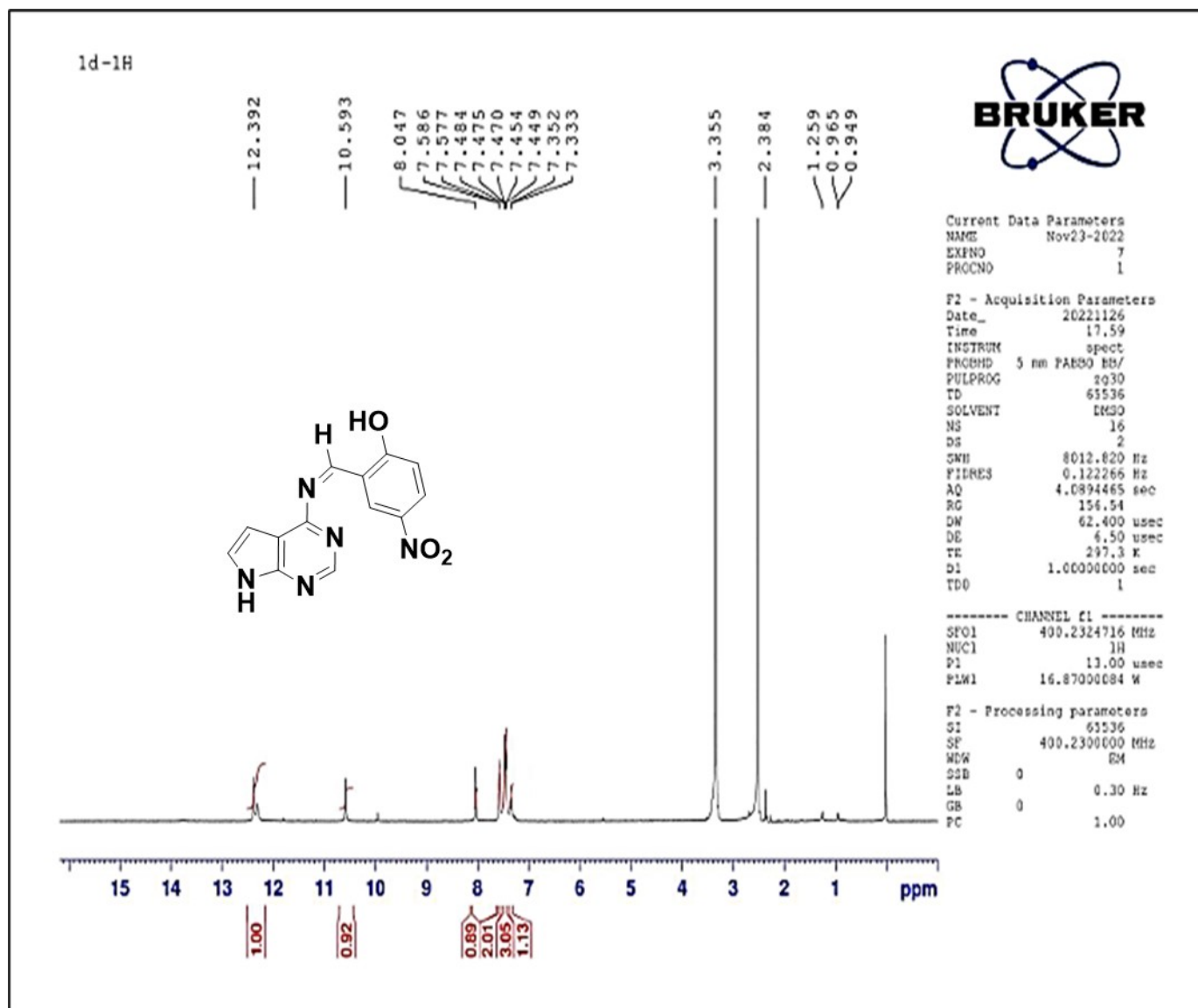


Figure. S8 ^1H NMR (400 MHz in DMSO-d_6) of the Compound APR1d: δ 12.392 (Ar-NH), δ 10.593 (Ar-OH), δ 8.047 (Ar-CH=NH), δ 7.333-7.586 (Ar-CH)

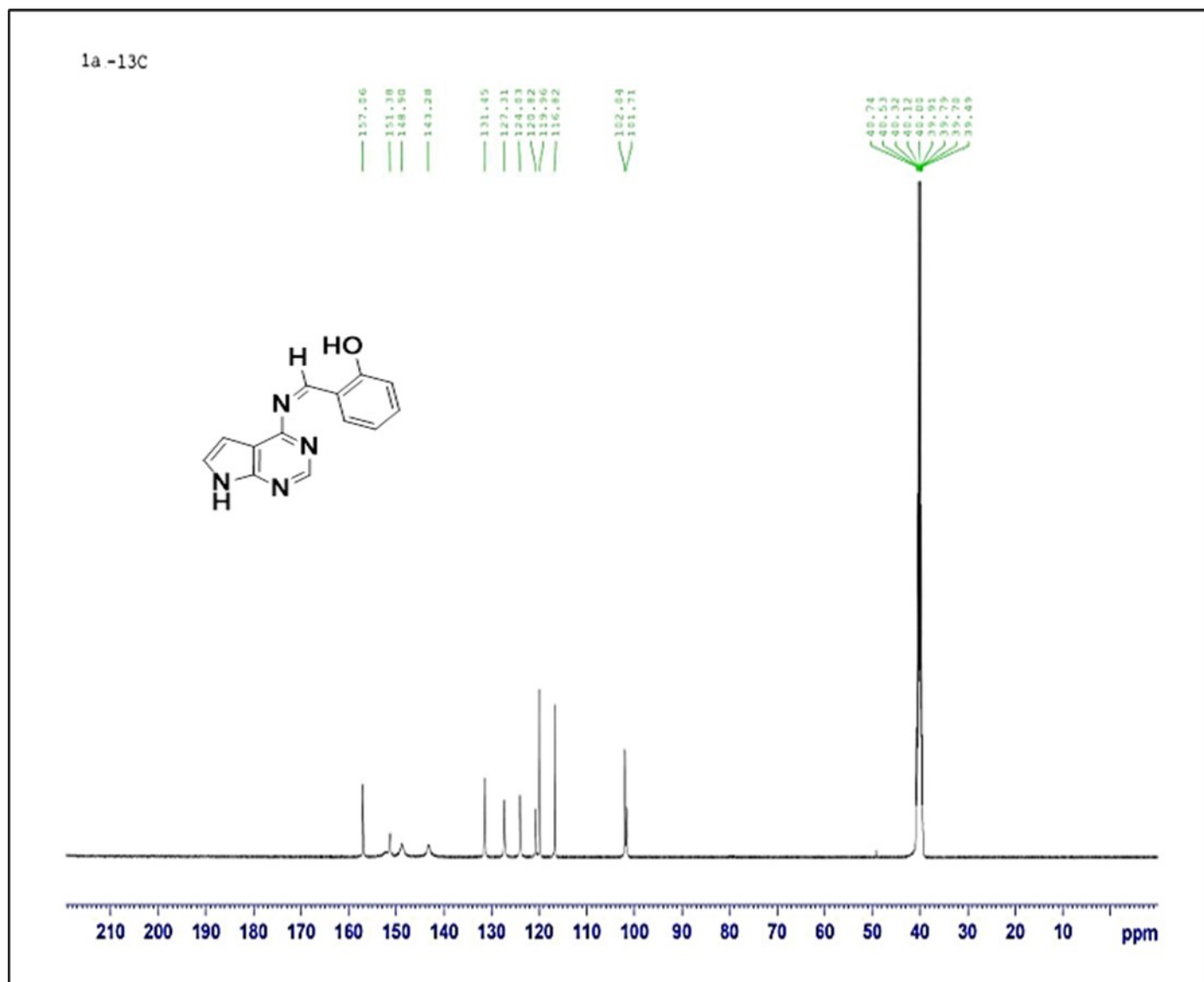


Figure. S9 ^{13}C NMR [400 MHz, DMSO- d_6 , $\delta(\text{ppm})$] of the Compound APR1a: 157.26 (-C=N imine carbon), 151.38 (Pyrimidine C between 2 N atom), 148.50 (Pyrimidine C to Adjust N group), 131.49 (-CH=), 120.02 (C1 Phenyl ring), 119.96 (C3 Phenyl ring), 116.02 (Pyrrole C₁), 104.04 (Pyrrole C₂), 101.71 (Pyrrole C₃)

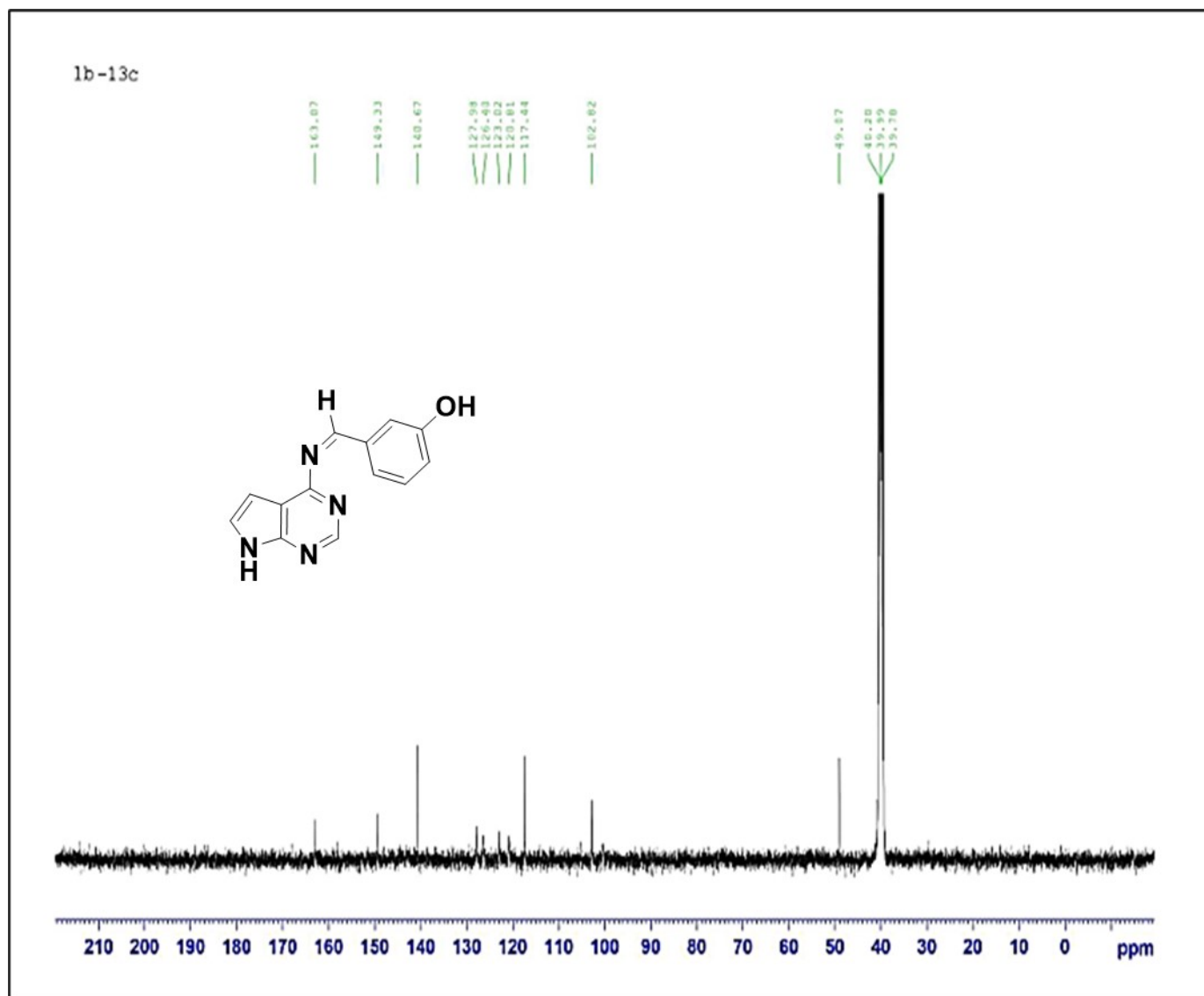


Figure. S10 ¹³C NMR [400 MHz, DMSO-d₆, δ(ppm)] of the Compound APR1b: 163.07 (-C=N imine carbon), 149.33 (Pyrimidine C between 2 N atom), 140.67 (Pyrimidine C to Adjust N group), 127.98 (-CH=), 126.48 (C1 Phenyl ring), 123.02 (C3 Phenyl ring), 120.01 (Pyrrole C₁), 117.44 (Pyrrole C₂), 102.02 (Pyrrole C₃)

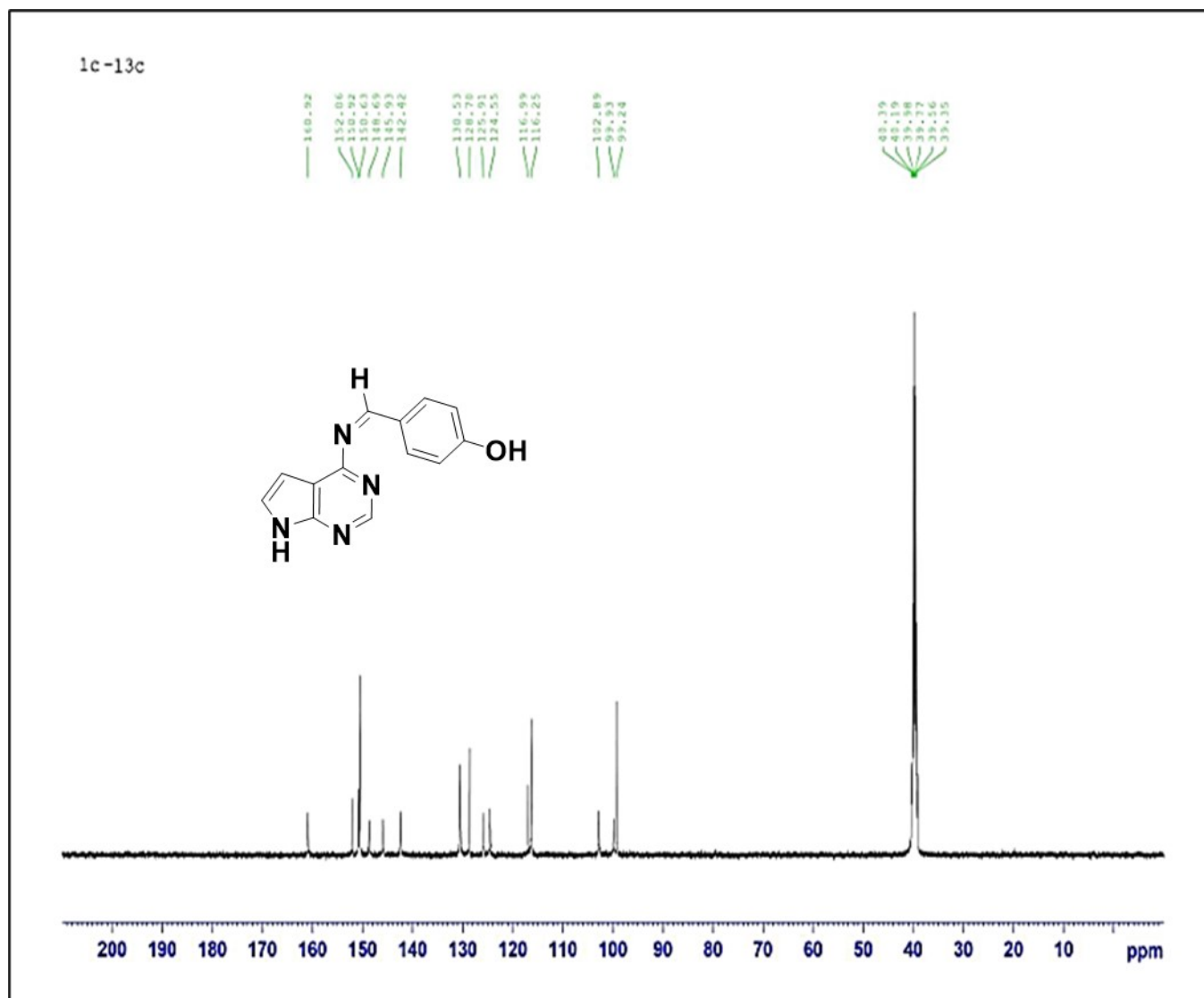


Figure. S11 ^{13}C NMR [400 MHz, DMSO- d_6 , $\delta(\text{ppm})$] of the Compound APR1c : 160.02 (-C=N imine carbon), 152.06 (Pyrimidine C between 2 N atom), 142.42 (Pyrimidine C to Adjust N group), 130.53 (-CH=), 126.78(C1 Phenyl ring), 124.55 (C3 Phenyl ring), 116.99 (Pyrrole C₁), 102.09 (Pyrrole C₂), 99.93 (Pyrrole C₃)

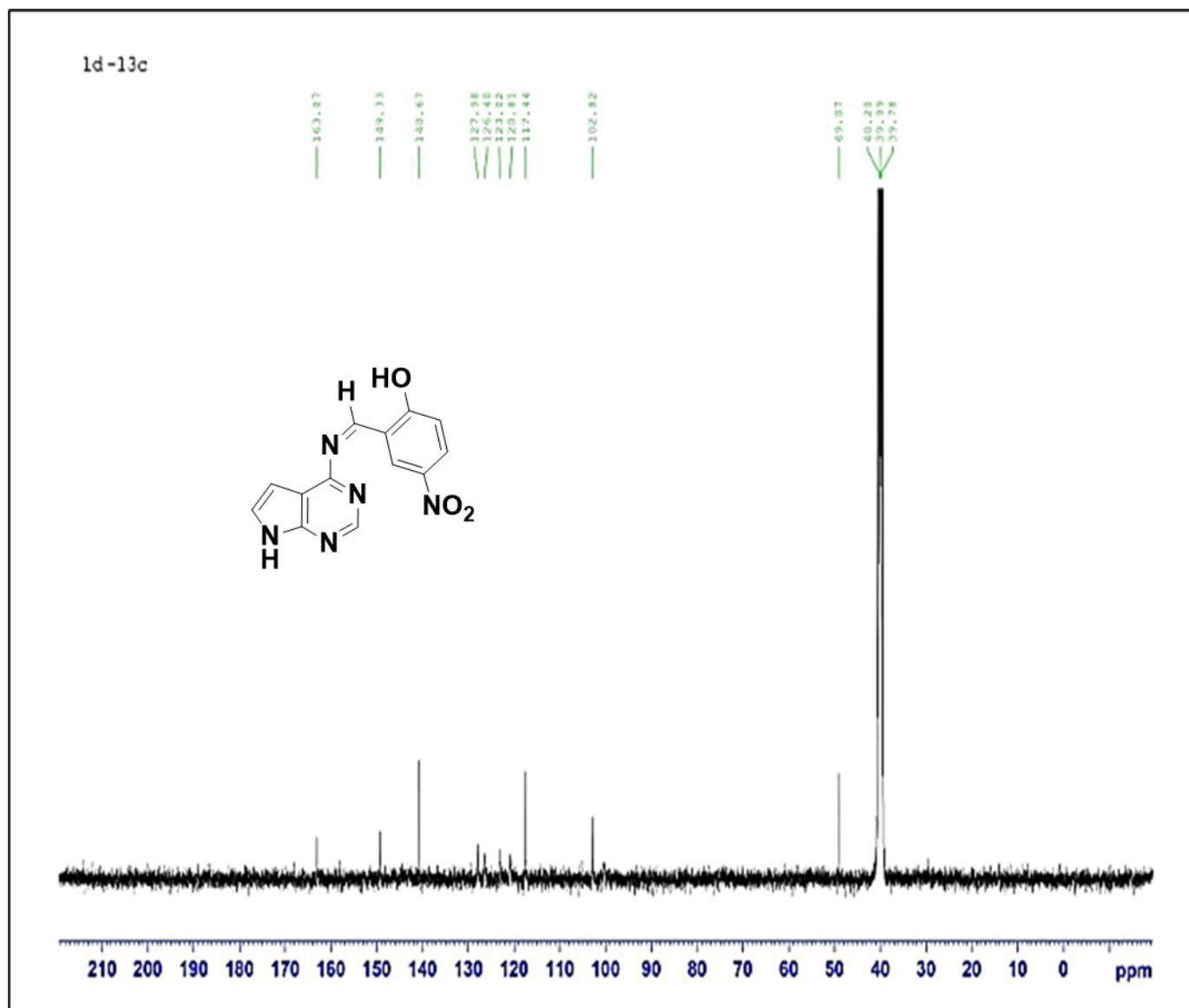


Figure. S12 ^{13}C NMR [400 MHz, DMSO-d_6 , $\delta(\text{ppm})$] of the Compound APR1d: 163.02 (-C=N imine carbon), 149.39 (Pyrimidine C between 2 N atom), 140.07 (Pyrimidine C to Adjust N group), 127.38 (-CH=), 126.40 (C1 Phenyl ring), 123.02 (C3 Phenyl ring), 120.01 (Pyrrole C₁), 117.40 (Pyrrole C₂), 102.02 (Pyrrole C₃)

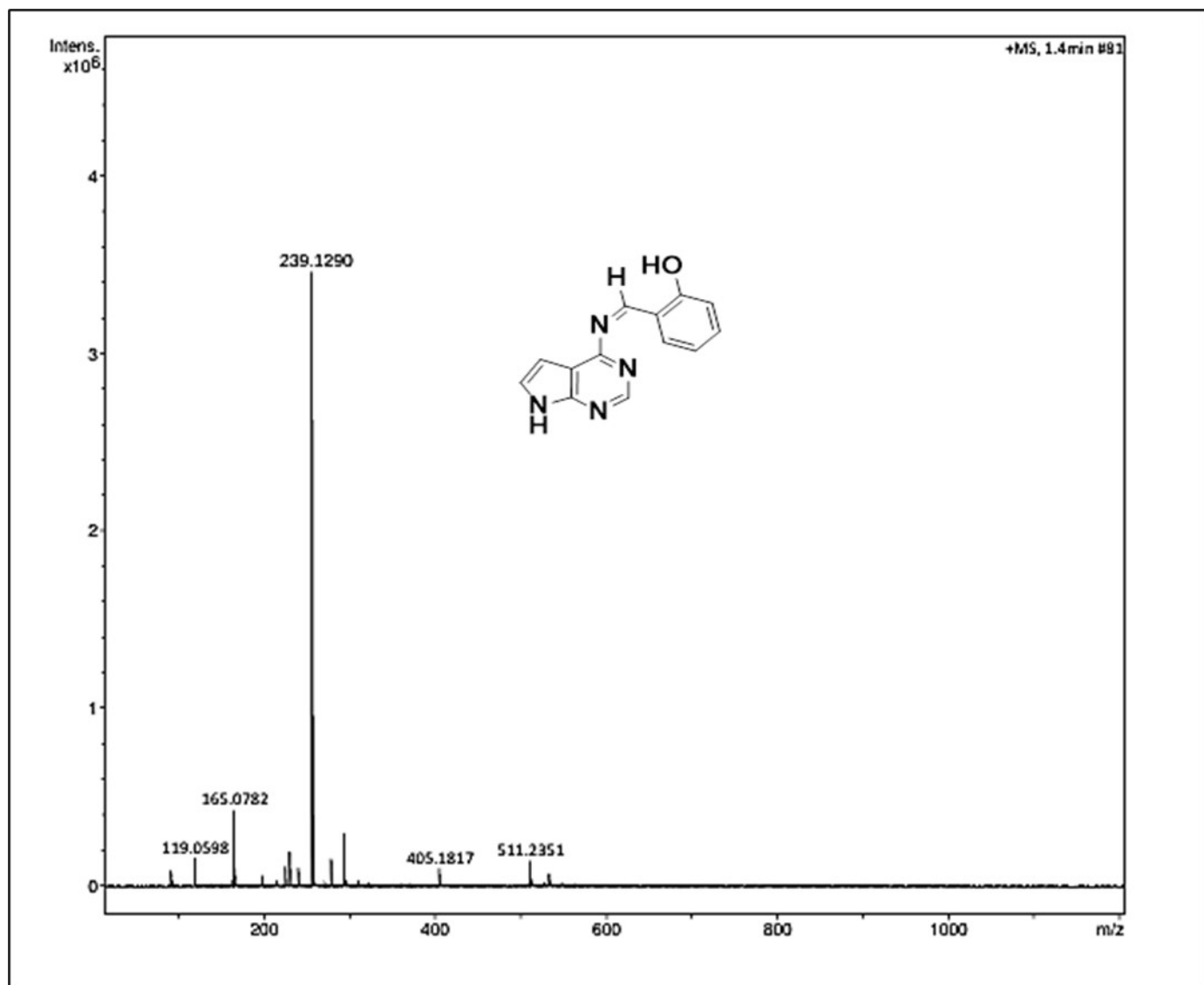


Figure. S13 MS spectrum of APR1a

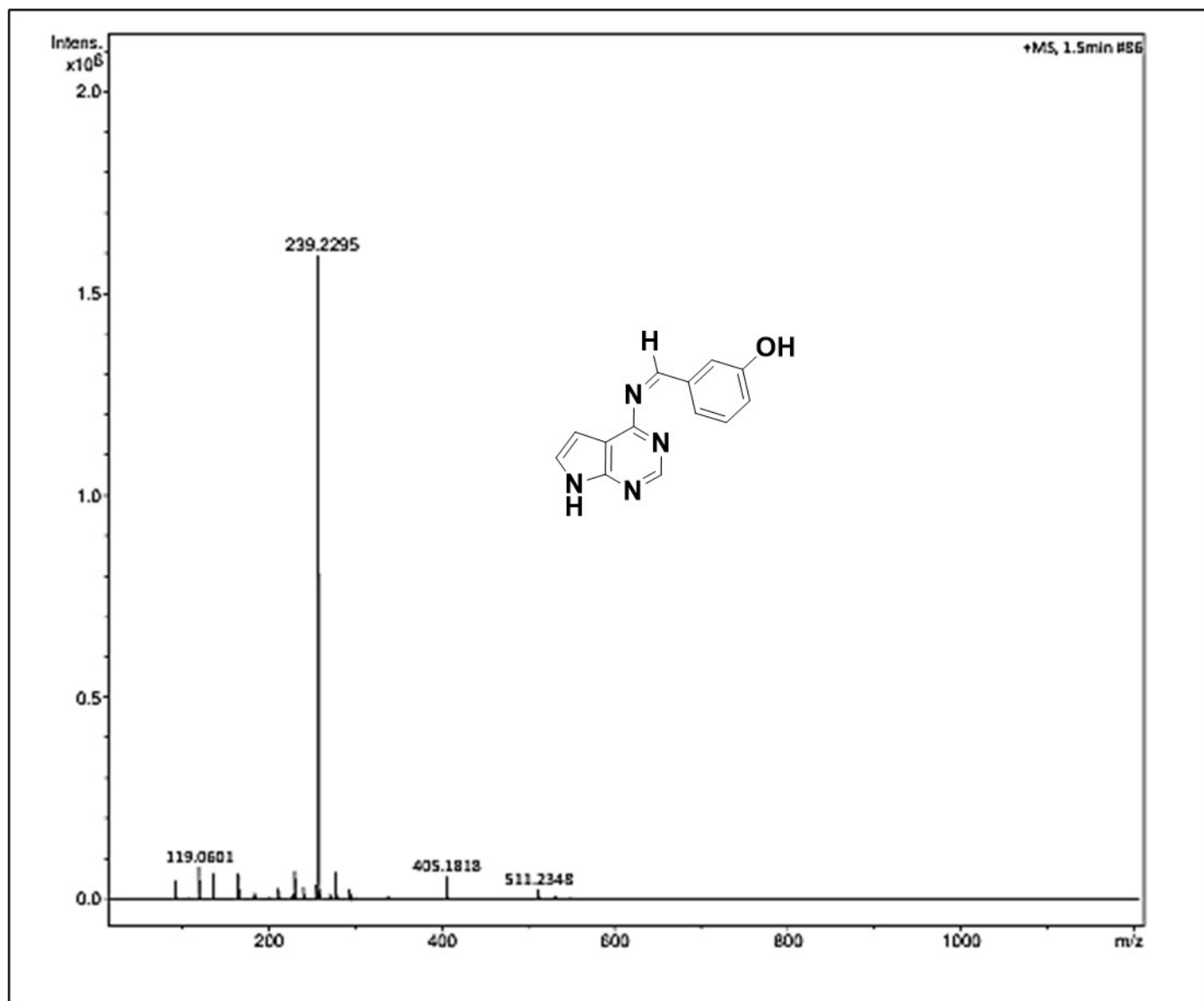


Figure. S14 MS spectrum of APR1b

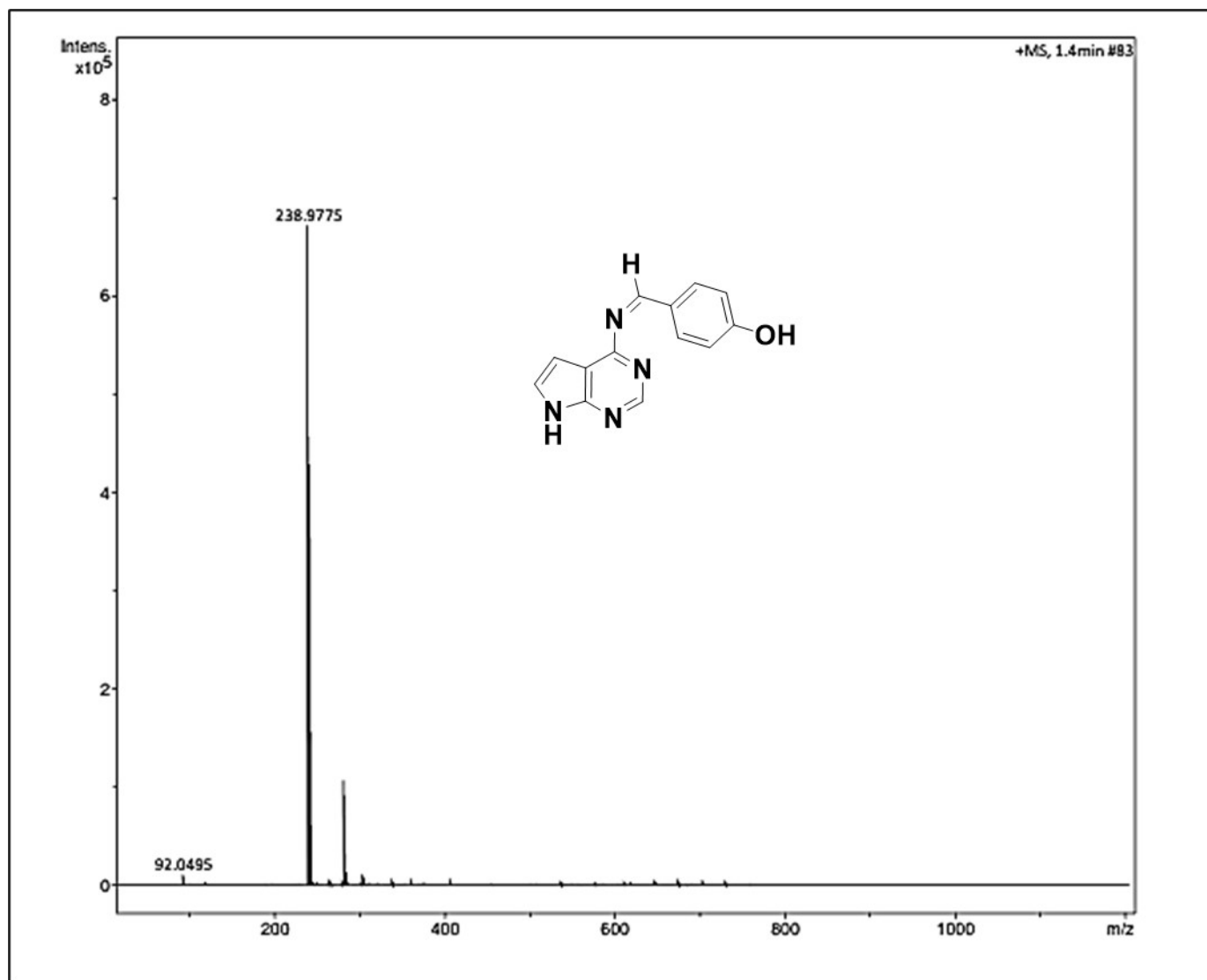


Figure. S15 MS spectrum of APR1c

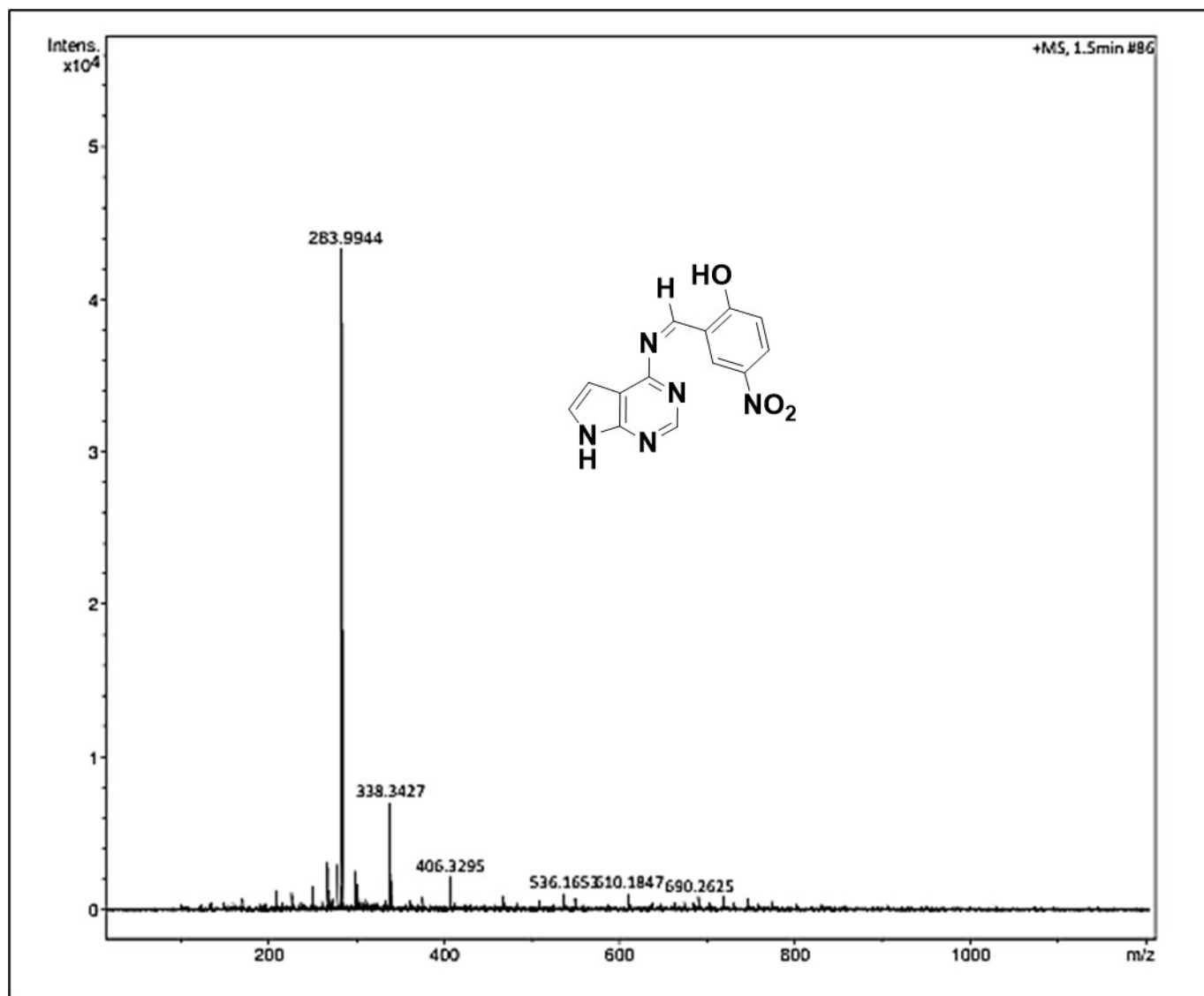


Figure. S16 MS spectrum of APR1d

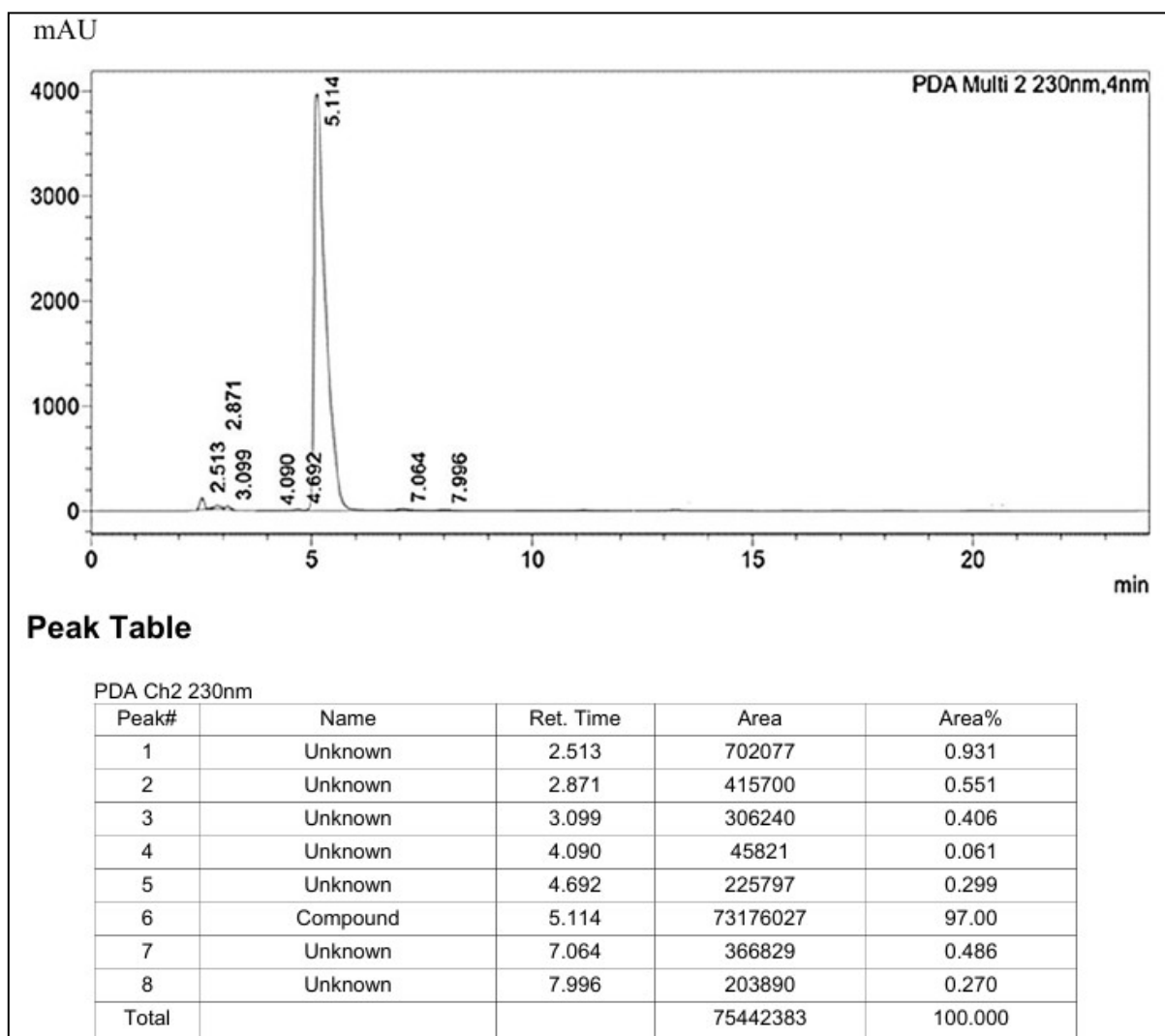
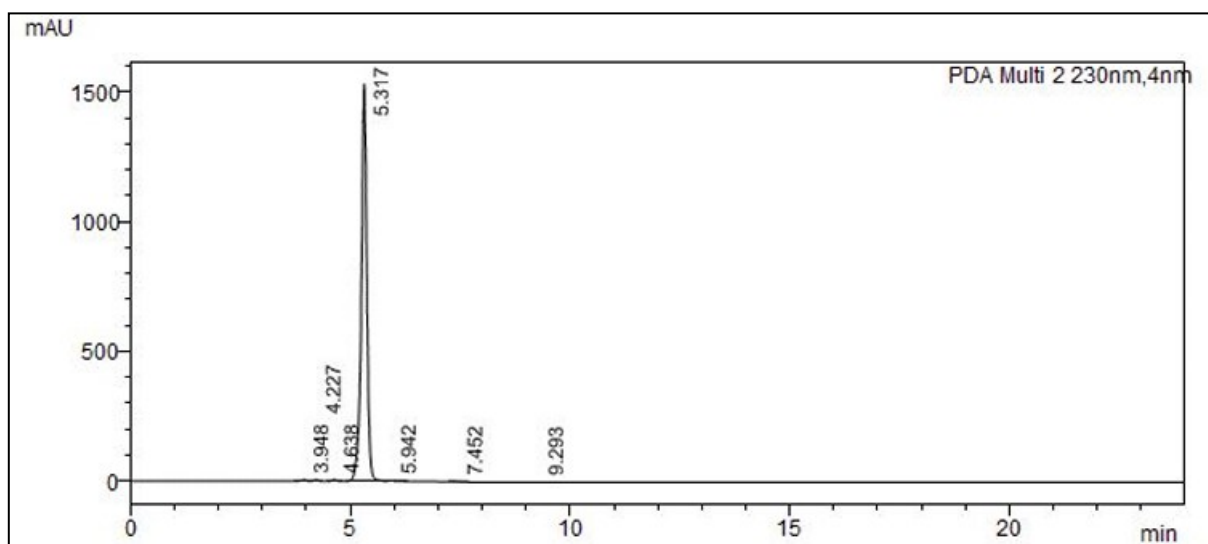


Figure. S17 HPLC Chromatogram of APR1a



Peak Table

PDA Ch2 230nm

Peak#	Name	Ret. Time	Area	Area%
1	Unknown	3.948	30420	0.224
2	Unknown	4.227	26103	0.192
3	Unknown	4.638	28359	0.209
4	Compound	5.317	13426241	98.989
5	Unknown	5.942	12978	0.096
6	Unknown	7.452	25442	0.188
7	Unknown	9.293	13872	0.102
Total			13563416	100.000

Figure. S18 HPLC Chromatogram of APR1b

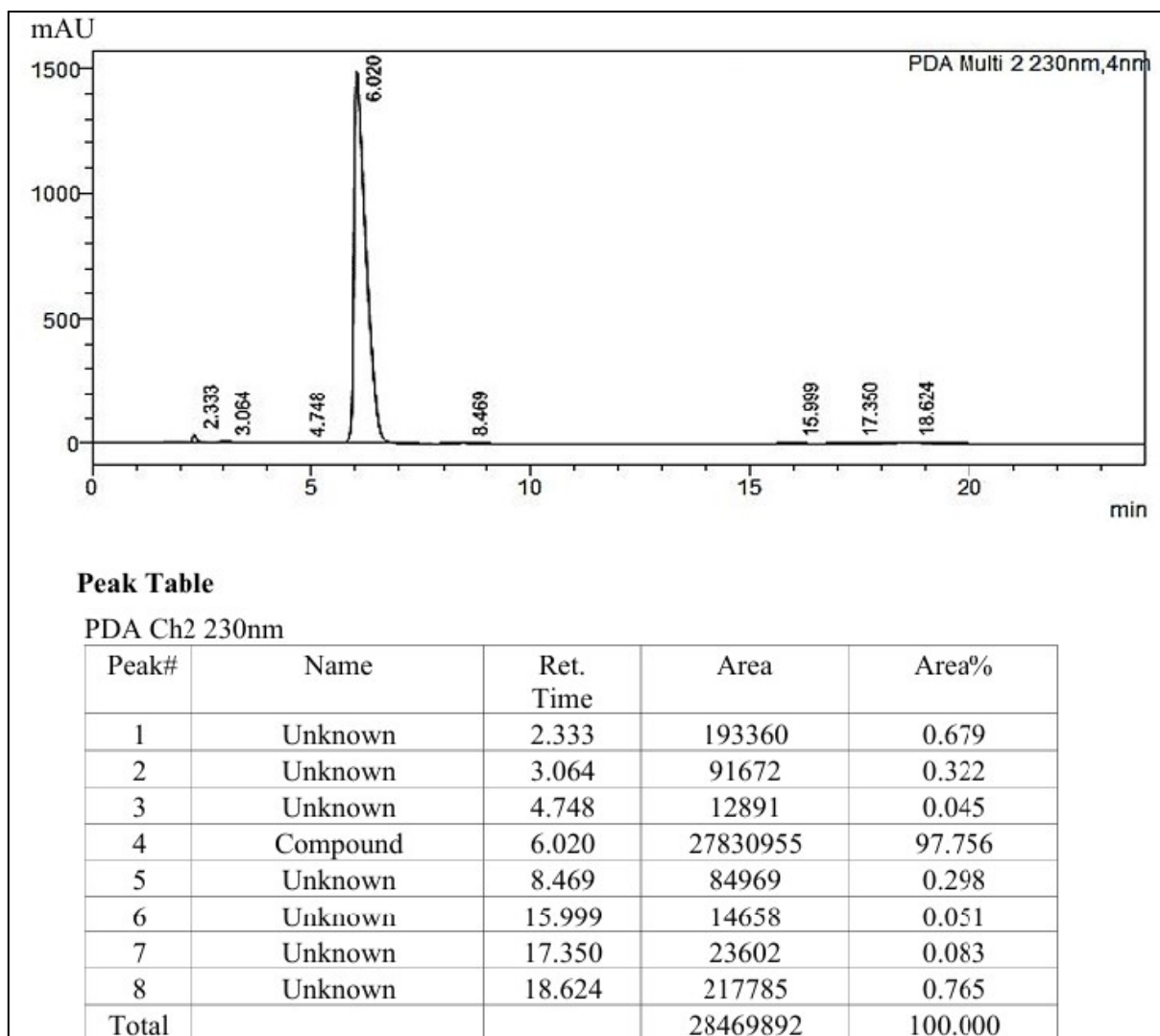


Figure. S19 HPLC Chromatogram of APR1c

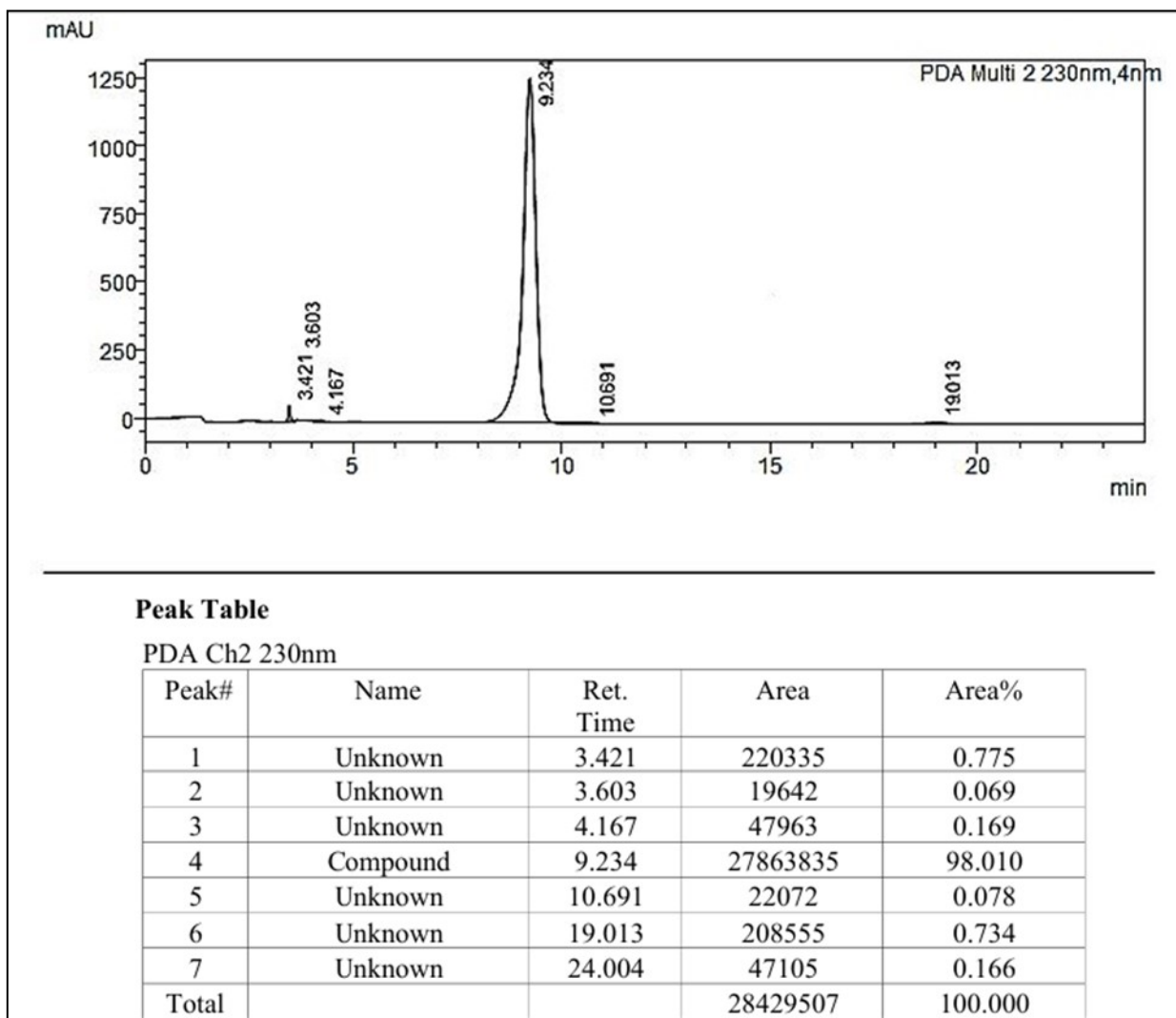


Figure. S20 HPLC Chromatogram of APR1d

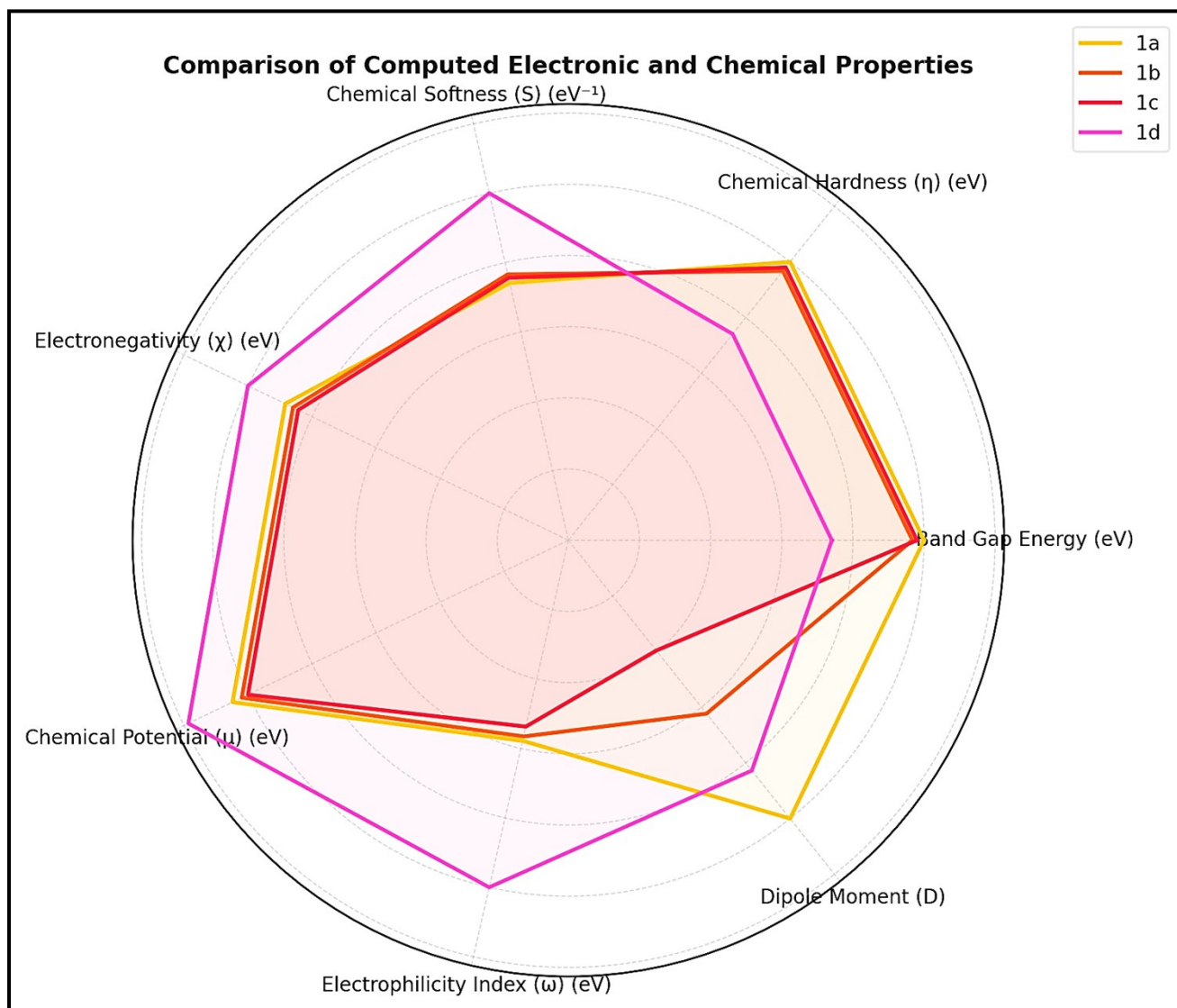


Figure S21. Comparison of computed electronic and chemical properties of synthesized compounds.

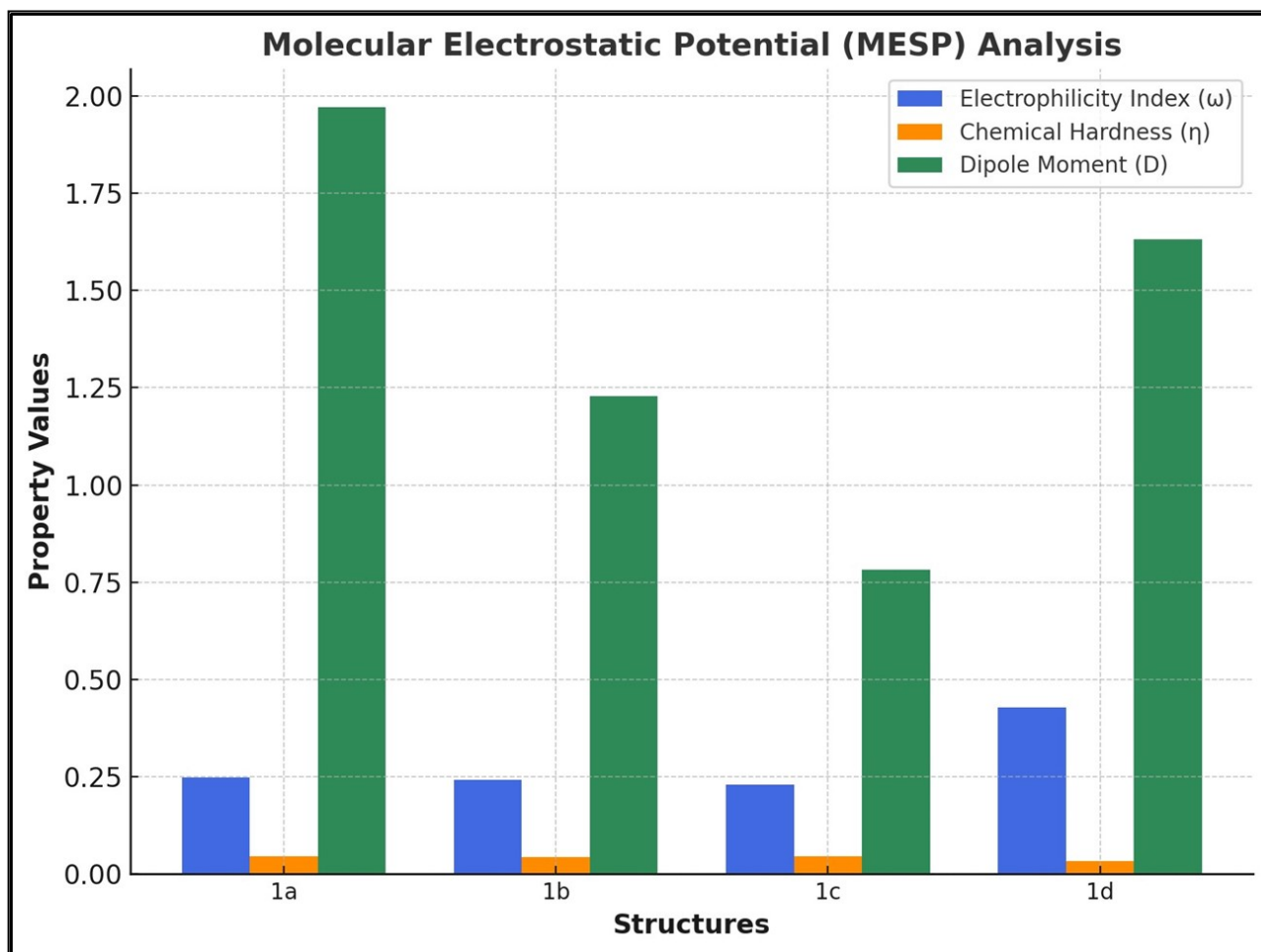


Figure S22. Molecular Electrostatic Potential analysis of synthesized compounds.

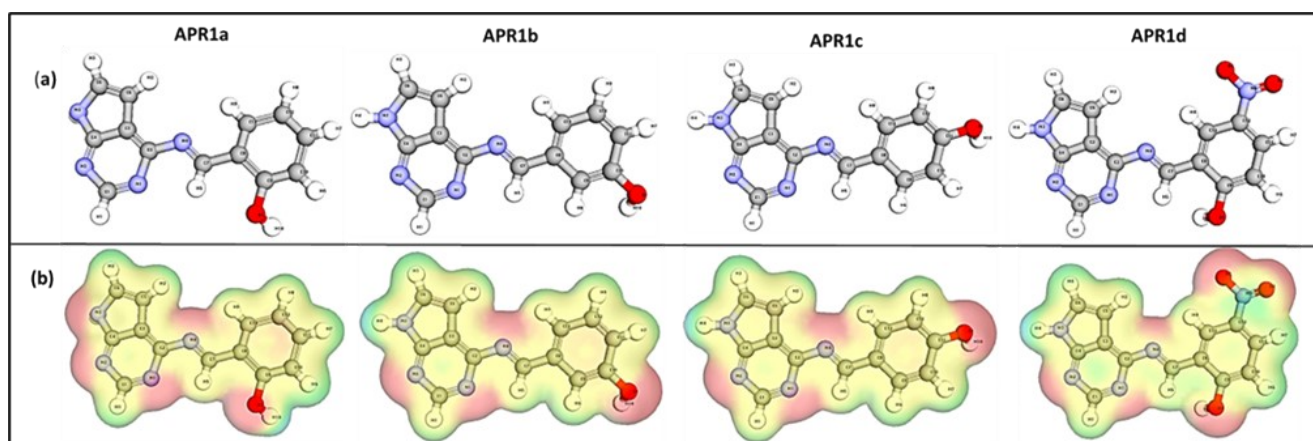


Figure S23. Optimized structures (a) of APR1a , APR1b, APR1c, APR1d ; Three-dimensional MESP (b) of APR1a , APR1b, APR1c, APR1d.

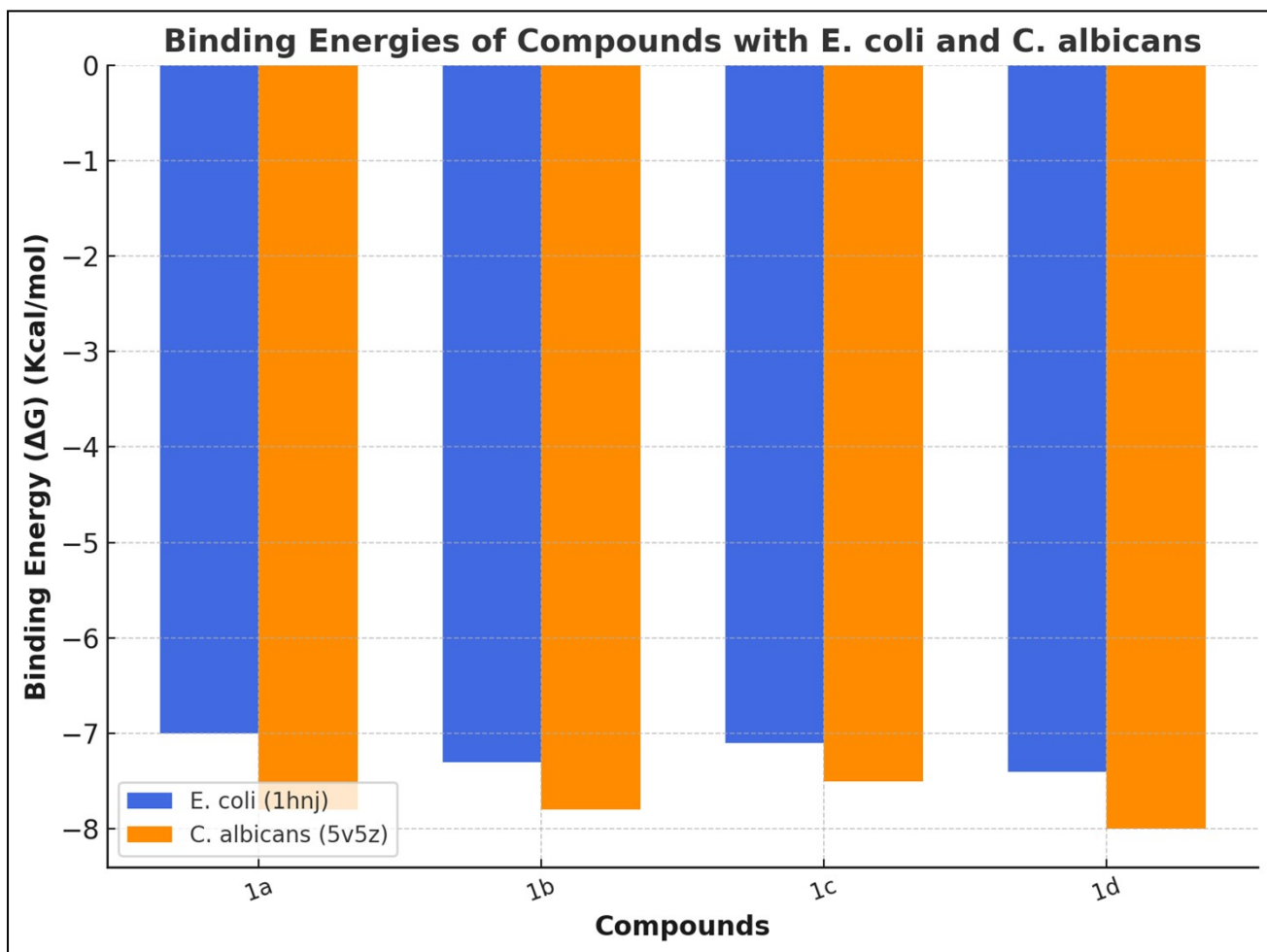
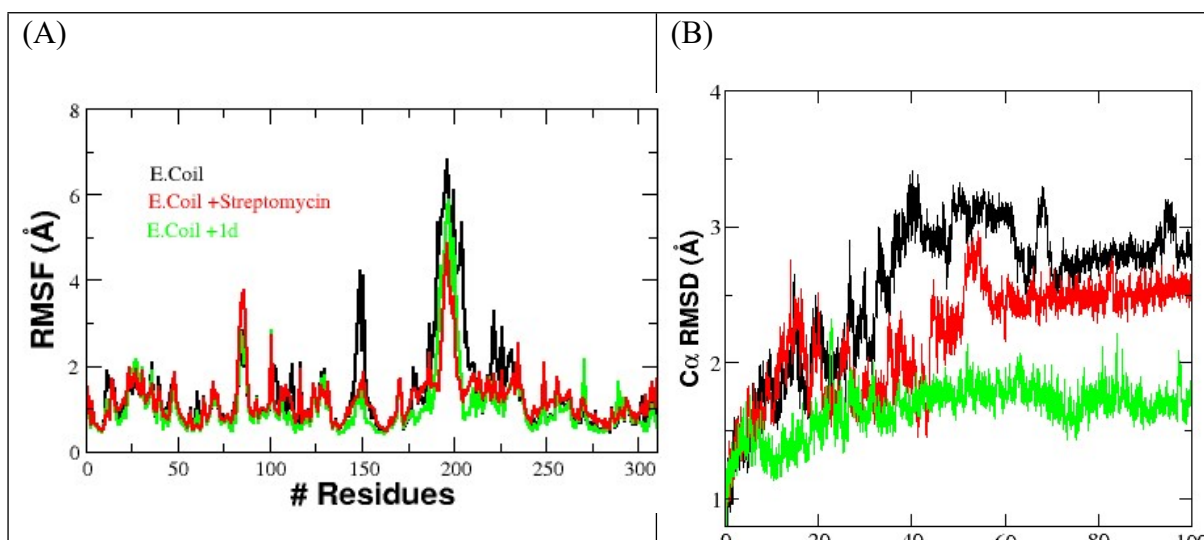
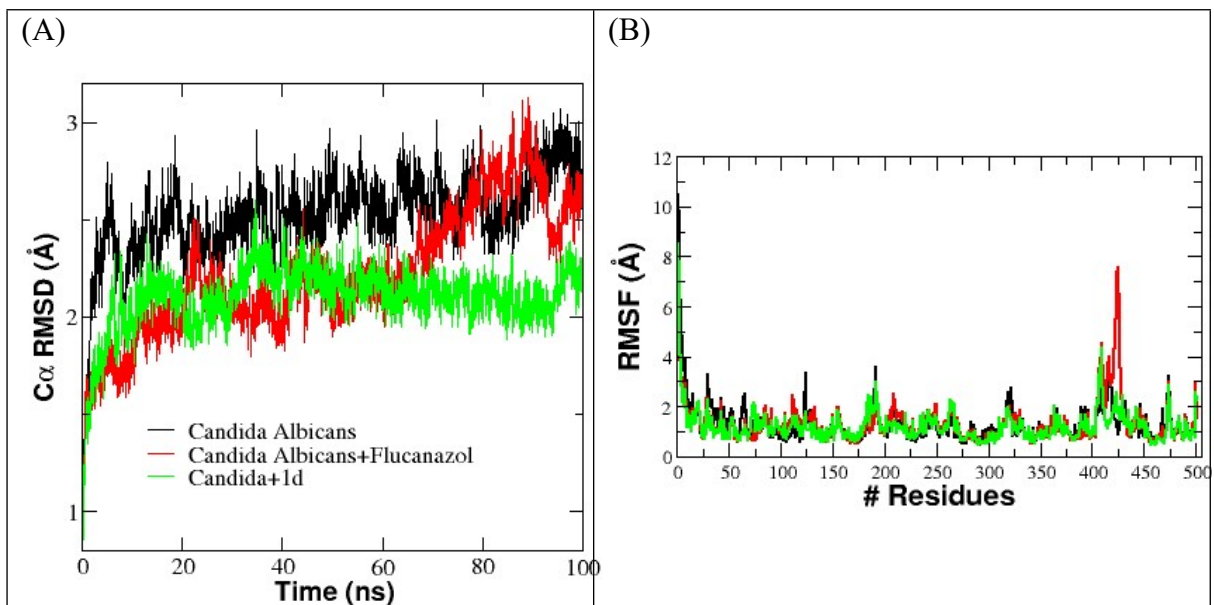
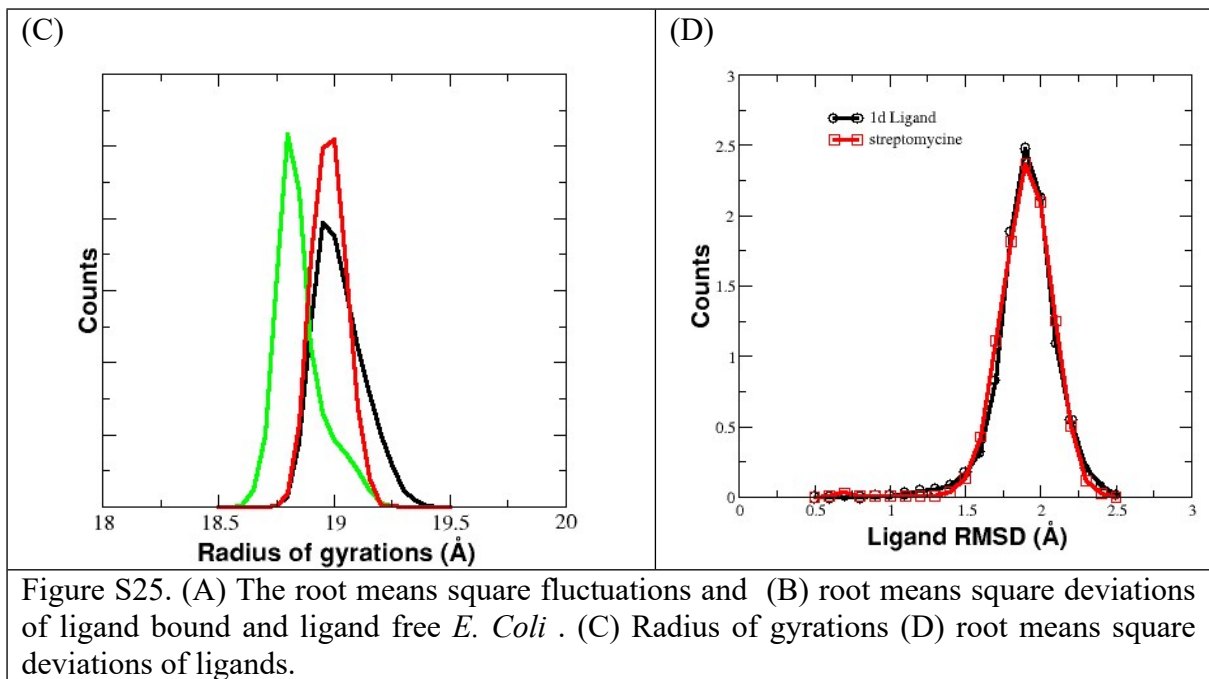


Figure S24. Binding energies of synthesised compounds (APR1a-d) with *E. coli* and *C. albicans*





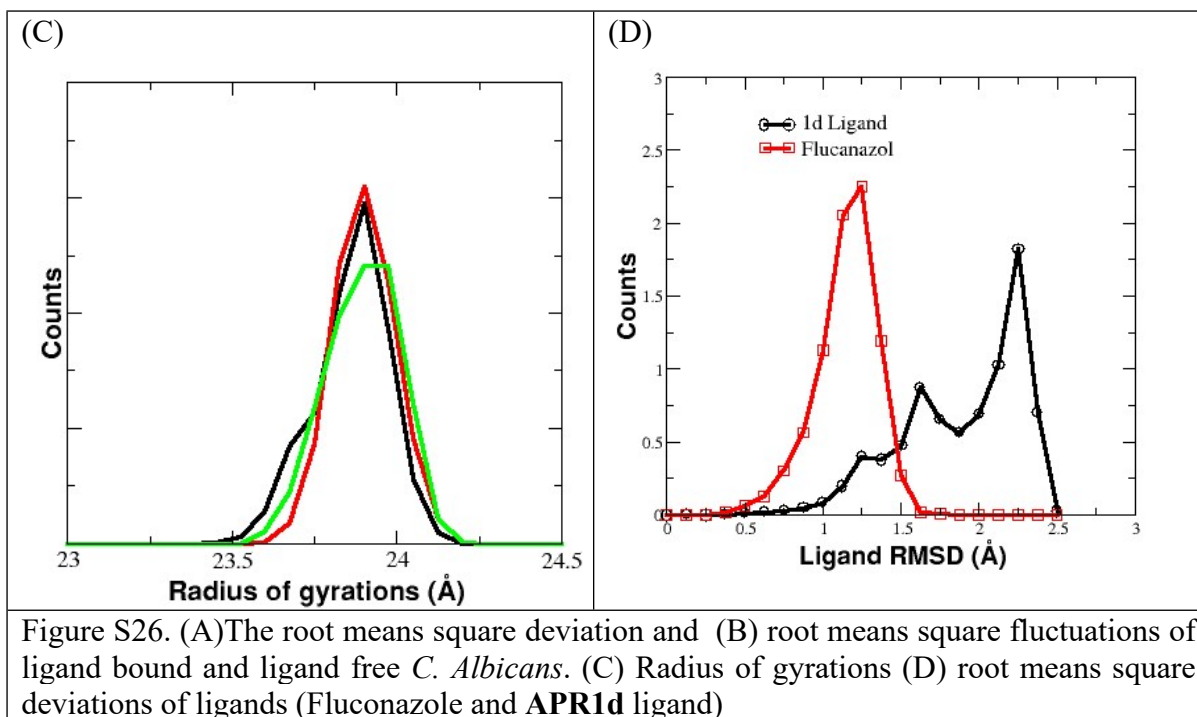


Figure S26. (A) The root means square deviation and (B) root means square fluctuations of ligand bound and ligand free *C. Albicans*. (C) Radius of gyration (D) root means square deviations of ligands (Fluconazole and APR1d ligand)

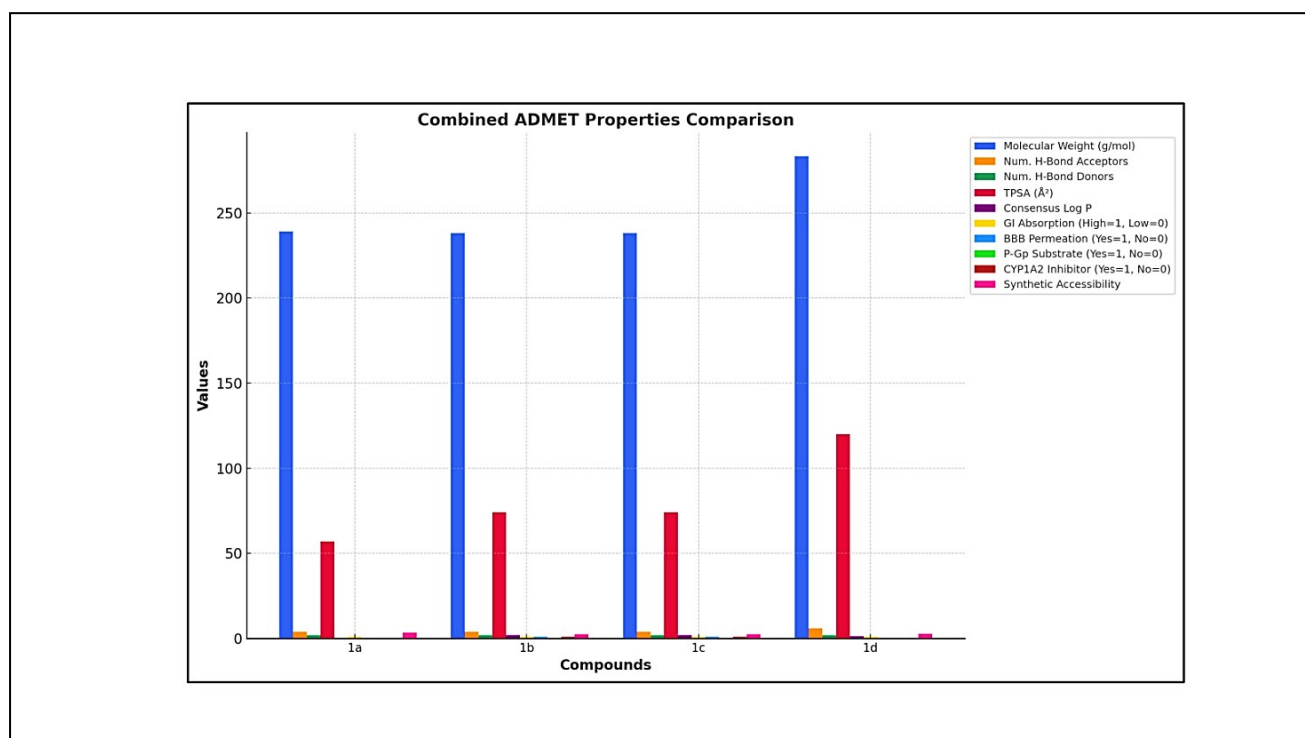


Figure S27. Combined ADMET properties comparison of the synthesized compounds.

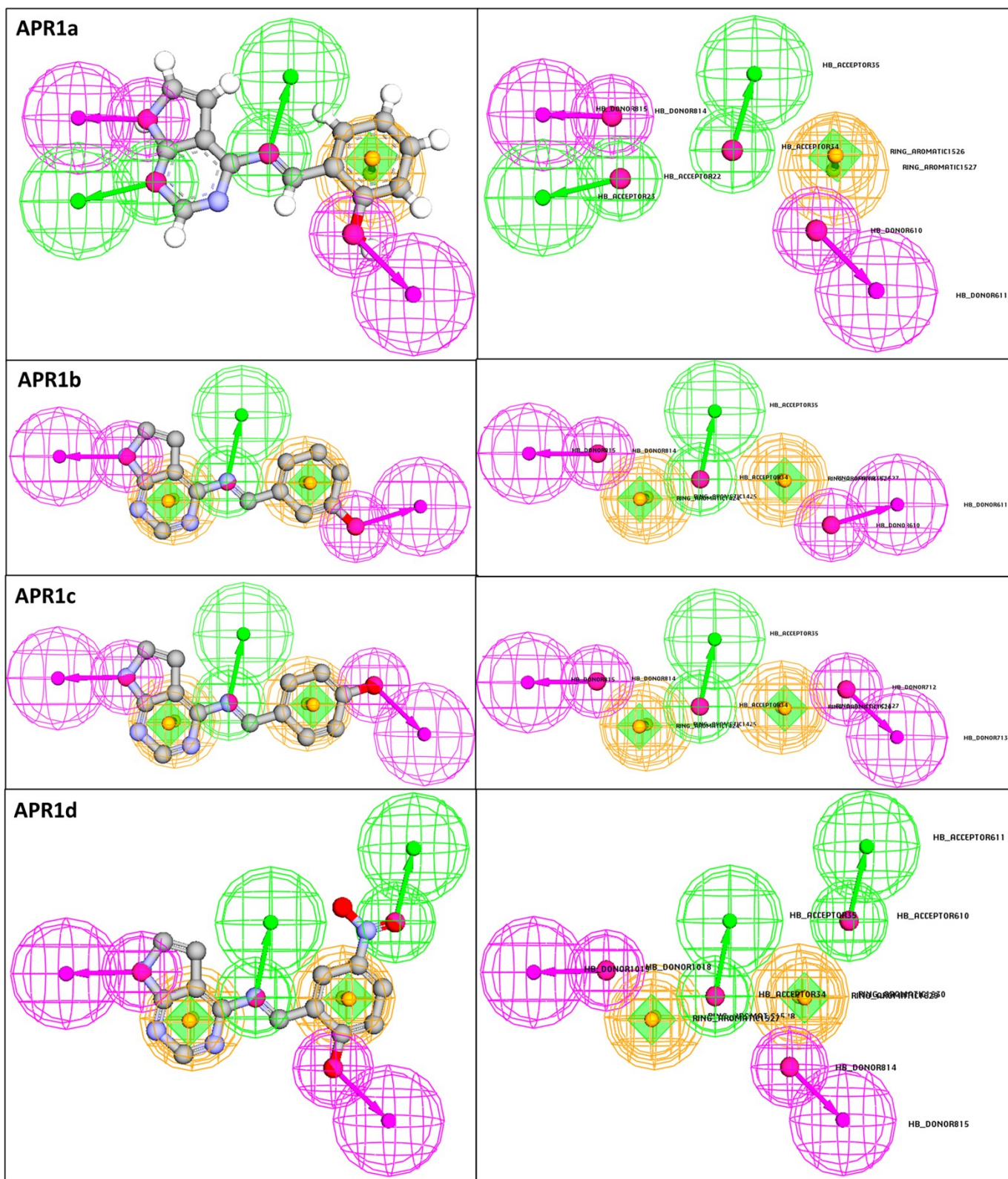


Figure S28. Structural and Molecular Interaction of synthesised compounds

Table S1. Antibacterial activities of synthesized compounds

Compound	Antibacterial Activity (zone of inhibition)				HPLC Purity (Area %)
	<i>S. aureus</i>	<i>B. subtilis</i>	<i>E. coli</i>	<i>P. aeruginosa</i>	
APR1a	21.5	7.5	15.0	16.0	97.00%
APR 1b	22.0	9.0	16.0	14.0	98.99%
APR 1c	25.0	11.0	17.0	18.5	97.76%
APR 1d	23.0	28.0	20.0	23.0	98.01%
<i>Streptomycin</i>	15.5	14.5	12.0	14.0	--

Table S2. Antifungal activities of synthesized compounds

Compound	<i>Candida albicans</i>	<i>Saccharomyces cerevisiae</i>	HPLC Purity (Area %)
APR1a	16.5	11.0	97.00%
APR 1b	12.5	15.5	98.99%
APR 1c	11.0	14.5	97.76%
APR 1d	19.0	19.0	98.01%
<i>Fluconazole</i>	10.5	14.0	--

Table S3. Brine shrimp bioassay of synthesized compounds

Compound	LC ₅₀ (M)	HPLC Purity (Area %)
APR1a	$>6.50 \times 10^{-4}$	97.00%
APR1b	$>3.50 \times 10^{-4}$	98.99%
APR1c	$>8.50 \times 10^{-4}$	97.76%
APR1d	$>4.50 \times 10^{-4}$	98.01%
<i>Vincristine Sulphate</i>	$>3.24 \times 10^{-4}$	--

Table S4. Computed Electronic and Chemical Properties of the Investigated Structures

Compounds	Total Energy (a.u.)	Binding Energy (eV)	HOMO Energy (eV)	LUMO Energy (eV)	Band Gap Energy (eV)	Chemical Hardness (η) (eV)	Chemical Softness (S) (eV ⁻¹)	Electronegativity (χ) (eV)	Chemical Potential (μ) (eV)	Electrophilicity Index (ω) (eV)	Dipole Moment (D)
APR1a	-788.649	-5.83885	-0.196596	-0.104948	0.091648	0.045824	10.9153	0.150772	-0.150772	0.247746	1.97171
APR 1b	-788.724	-5.91375	-0.190962	-0.102282	0.088680	0.044340	11.2792	0.146622	-0.146622	0.242446	1.22855
APR 1c	-788.726	-5.91646	-0.188788	-0.098933	0.089855	0.044928	11.1282	0.143861	-0.143861	0.230262	0.781615
APR 1d	-991.781	-6.27115	-0.204577	-0.136667	0.067909	0.033954	14.7216	0.170622	-0.170622	0.428791	1.63151

Table S5. Molecular Electrostatic Potential (MESP) Analysis of Investigated Structures

Structure	Electrostatic Potential Distribution	Key Reactive Sites	Charge Distribution	Predicted Reactivity	Potential Applications
APR1a	Well-distributed, moderate negative potential near electronegative atoms (O, N).	Oxygen and nitrogen atoms.	High dipole moment (1.97 D), suggesting strong polarity.	Strong hydrogen bonding interactions, good nucleophilicity.	Drug-receptor interactions, molecular recognition in biological systems.
APR1b	Uniform electrostatic potential gradient, moderate charge separation.	Moderate electron-rich and electron-deficient zones.	Balanced charge distribution, slightly lower dipole moment (1.23 D).	Selective molecular interactions, stable reactivity.	Enzyme inhibition, selective binding in drug design.
APR1c	Less polarized MESP, more uniform charge distribution.	Weak nucleophilic and electrophilic regions.	Lowest dipole moment (0.78 D), indicating minimal charge separation.	Moderate reactivity, reduced hydrogen bonding ability.	Solid-state applications, packing efficiency in materials science.
APR1d	Strong localized negative potential, intense electrostatic variations.	Highly nucleophilic regions around electronegative atoms.	Highest electrophilicity (0.4288 eV), lowest chemical hardness (0.0339 eV).	Most reactive structure , strong charge transfer potential.	Catalysis, charge-transfer materials, bioactive molecule development.

Table S6. Binding Energies, Hydrogen Bonding, and Steric Interactions of Compounds with *E. coli* (PDB: 1hnj) and *Candida albicans* (PDB: 5v5z)

Compounds	Binding Energy (Kcal/Mol) (Delta G)	Hydrogen Bond	Steric Interactions
E.Coli (PDB: 1hnj)			
APR1a	-7.0	Ala246, Asn247	Ala246, Asn247
APR 1b	-7.3	Asn247	Ala246, Asn247
APR1c	-7.1	--	Asn247
APR 1d	-7.4	Phe304	Asn210, Arg249, Ile250, Phe304
Streptomycin (Control)	-6.2	Asp150, Gly152, Met207, Gly209, Asn210	Arg36, Asp150, Met207, Gly209, Asn210
Candida Albicans (PDB: 5v5z)			
APR1a	-7.8		

APR1b	-7.8	Tyr118	Tyr118, Phe463
APR1c	-7.5	--	His377, Ser378
APR1d	-8.0	His377, Ser378	Gly307, His377, Ser378
Fluconazole (Control)	-7.8	Ile304, Thr311	Leu204, Leu276, Ile304, Gly308, Thr311, Gly472

Table S7. Binding free energy values of *Streptomycin* with *E. Coli*

Binding free energy components of <i>E. Coli</i> and <i>Streptomycin</i>	
ΔE_{ELEC}	-24.6
ΔE_{VDW}	-16.0
ΔEPB	33.0
$\Delta \text{EPB}_{\text{np}}$	-2.5
ΔE_{Disper}	0.0
ΔG	-9.63±3.2

Binding free energy (ΔG) of *E. Coli protein* and ligand complex was calculated from the 100 ns simulation. The molecular-mechanical energy calculations were performed using MM/PBSA, and entropy calculations using nmode analysis. ΔE_{ELEC} , ΔE_{VDW} , $\Delta \text{EPB}_{\text{np}}$ and $\Delta \text{EPB}_{\text{solv}}$ are referred to the electrostatic, Vander Waals, polar, the non-polar contribution to the solvation energy and the electrostatic contribution to the solvation energy, respectively.

Table S8. Binding free energy values of **APR1d** ligand with *Candida Albicans* protein

Binding free energy components of <i>Candida Albicans</i> protein and APR1d ligand	
ΔE_{ELEC}	000
ΔE_{VDW}	-39.41
ΔEPB	11.37
$\Delta \text{EPB}_{\text{np}}$	-0.82
ΔE_{Disper}	0.0
$\Delta G(\Delta H_{\text{PB}} - T\Delta S)$	-28.8±3.2

Binding free energy (ΔG) of *Candida Albicans* protein and ligand complex was calculated from the 100 ns simulation. The molecular-mechanical energy calculations were performed using MM/PBSA, and entropy calculations using nmode analysis. ΔE_{ELEC} , ΔE_{VDW} , $\Delta \text{EPB}_{\text{np}}$ and $\Delta \text{EPB}_{\text{solv}}$ are referred to the electrostatic, Vander Waals, polar, the non-polar contribution to the solvation energy and the electrostatic contribution to the solvation energy, respectively.

Table S9. Binding free energy values of *Fluconazol* with *Candida Albicans* protein

Binding free energy components of <i>Candida Albicans</i> protein and <i>Fluconazol</i>	
ΔE_{ELEC}	-29.12

ΔE_{VDW}	-35.92
ΔEPB	42.21
ΔEPB_{np}	-3.42
ΔE_{Disper}	0.0
$\Delta G(\Delta H_{PB}-T\Delta S)$	-25.8±3.2

Binding free energy (ΔG) of Candida Albicans protein and ligand complex was calculated from the 100 ns simulation. The molecular-mechanical energy calculations were performed using MM/PBSA, and entropy calculations using nmode analysis. ΔE_{ELEC} , ΔE_{VDW} , ΔEPB_{np} and ΔEPB_{solv} are referred to the electrostatic, Vander Waals, polar, the non-polar contribution to the solvation energy and the electrostatic contribution to the solvation energy, respectively

Table S10. ADMET Calculations

Parameters	APR1a	APR1b	APR1c	APR1d
PHYSICOCHEMICAL PROPERTY				
Formula	C13H11N4O	C13H10N4O	C1H10N4O	C13H9N5O3
MW (G /Mol)	239.25	238.24	238.24	283.24
Num. Heavy Atoms	18	18	18	21
Num. arom. Heavy Atoms	6	15	15	15
Fraction Csp3	0.08	0.00	0.00	0.00
Num. Of Rotatable Bonds	2	2	2	3
Num. H-Bond Acceptors	4	4	4	6
Num. H-Bond Donors	2	2	2	2
Molar Refractivity	83.25	69.61	69.61	78.43
TPSA (A²)	56.98	74.16	74.16	119.98
LIPOPHILICITY				
Log P_{o/w} (Ilogp)	0.00	1.65	1.65	1.04
Log P_{o/w} (XLOGP3)	-0.73	1.94	1.94	1.77
Log P_{o/w} (WLOGP)	-0.90	2.41	2.41	2.32
Log P_{o/w} (MLOGP)	0.93	1.25	1.25	0.33
Log P_{o/w} (SILICOS-IT)	1.40	2.85	2.85	0.66
Consensus Log P_{o/w}	0.14	2.02	2.02	1.22
WATER SOLUBILITY				
Log S (ESOL)	-0.98	-3.02	-3.02	-3.04
Solubility Class	Very soluble	Soluble	Soluble	Soluble
Log S (ALI)	0.01	-3.12	-3.12	-3.91
Solubility Class	Highly soluble	Soluble	Soluble	Soluble
Log S (SILICOS-IT)	-3.22	-4.58	-4.58	-3.95
Solubility Class	soluble	Moderately soluble	Moderately soluble	Soluble
PHARMACOKINETICS				
GI Absorption	High	High	High	High
BBB Permeation	No	Yes	Yes	No
P-Gp Substrate	No	No	No	No
CYP1A2 Inhibitor	No	Yes	Yes	No

CYP2C19 Inhibitor	No	No	No	No
CYP2C9 Inhibitor	No	No	No	No
CYP2D6 Inhibitor	No	No	No	No
CYP3A4 Inhibitor	No	No	No	No
Log K_p (Skin Permeation) cm/s	-8.28	-6.38	-6.38	-6.77
DRUG LIKENESS				
Lipinski	Yes: 0 violation	Yes: 0 violation	Yes: 0 violation	Yes: 0 violation
Ghose	No: 1 violation	Yes	Yes	Yes
Veber	Yes	Yes	Yes	Yes
Egan	Yes	Yes	Yes	Yes
Muegge	Yes	Yes	Yes	Yes
Bioavailability Score	0.55	0.55	0.55	0.55
MEDICINAL CHEMISTRY				
PAINS	0 alert	0 alert	0 alert	0 alert
Brenk	1 alert: imine_1	1 alert: imine_1	1 alert: imine_1	3 alert: imine_1, nitro_group, oxygen-nitrogen_single bond
Leadlikeness	No; 1 violation; MW<250	No; 1 violation; MW<250	No; 1 violation; MW<250	Yes
Synthetic Accessibility	3.43	2.53	2.50	2.77

Table S11. Hydrogen Bonding, Hydrophobicity, and Aromaticity Profile of the Compounds

Compound	Hydrogen Bond Acceptor	Hydrogen Bond Donor	Hydrophobic	Ring Aromatic	Negative Ionizable	Positive Ionizable
1a	5	3	2	6	--	--
1b	5	3	2	6	--	--
1c	5	3	2	6	--	--
1d	7	3	1	6	--	--

